



Cite this: *Energy Adv.*, 2024, 3, 366

Received 9th August 2023,  
Accepted 17th December 2023

DOI: 10.1039/d3ya00389b

rsc.li/energy-advances

## Improving plastic pyrolysis oil quality via an electrochemical process for polymer recycling: a review

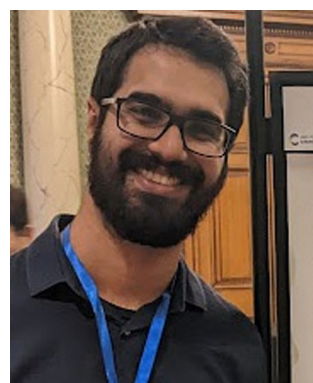
César Catizane, Ying Jiang \* and Joy Sumner

Electrochemical hydrogenation (ECH) is a novel route for the upgradation of pyrolysis oil from both biomass and plastic feedstocks. Compared with conventional routes, including thermal cracking, ECH can be performed under mild conditions (< 80 °C and 1 atm) and without the requirement of additional H<sub>2</sub> supply. The successful demonstration of this application can be a critical step to enabling a circular plastic economy and low-carbon fuel production. In this review we provide a critical overview of the recent advancements in understanding the variables that influence the ECH process. In addition, we debate how this technology could be optimized and applied to plastic waste pyrolysis oil, assessing concerns such as the selection of cathode material, which needs to be resilient enough to address the complex nature of bio-oil. In addition, we present ideas on how to circumvent the challenge where the commonly used water-based electrolytes are unlikely to be suitable for pyrolysis oil treatment. Finally, we discuss the possible utilization of this product and scalability of this process.

## 1 Introduction

With the increasing severity of climate change and global warming, there is a growing recognition for the pressing need

*School of Water, Energy and Environment, Cranfield University, College Rd, Cranfield, Wharley End, Bedford, UK. E-mail: y.jiang@cranfield.ac.uk*



César Catizane

steam reforming. César also has a history working with both companies and government agencies, in an effort to help them achieve their carbon neutral goals.

to mitigate carbon emissions and other greenhouse gases. To address this environmental challenge, several key international targets and agreements have been established, including Agenda 2030 and the Paris agreement. The United Nations' Agenda 2030 has outlined a set of sustainable development goals (SDGs). These goals encompass the effective management of waste, the preservation of ocean ecosystems, and the urgent

*César graduated from Pontifical Catholic University, Brazil, in Chemical Engineering and is now a PhD student at Cranfield University. His project is focused on evaluating the extent to which electrochemistry can be used to improve the pyrolysis oil quality and processing in feedstock recycling plants. He has carried out projects focused on wastewater treatment via electrochemistry and production of hydrogen from ethanol, utilizing*

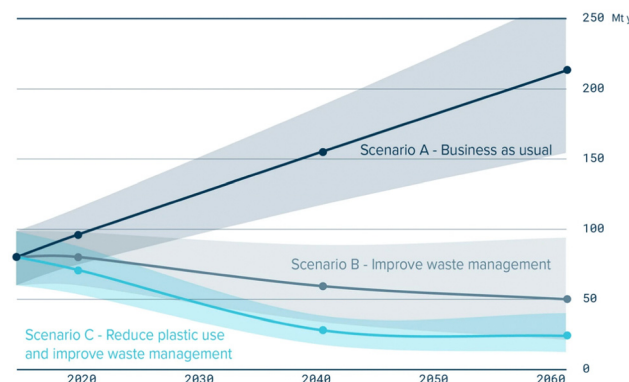


Ying Jiang

*Dr Ying Jiang is a Senior Lecturer in Bioenergy within the School of Water, Energy and Environment. Ying has extensive experiences in developing research programmes to improve the technical viability of biofuel production processes and maintain a consistent product quality and higher reaction kinetics. Current he leads the bioenergy research activities at Cranfield University, focusing on the fundamental reactions involved in biochemical and thermo-chemical conversion routes of biomass/waste to energy. This scientific enquiry is key to address the demand of the bioenergy sector for an improved technical viability of biofuel production processes, consistent product quality and higher reaction kinetics.*

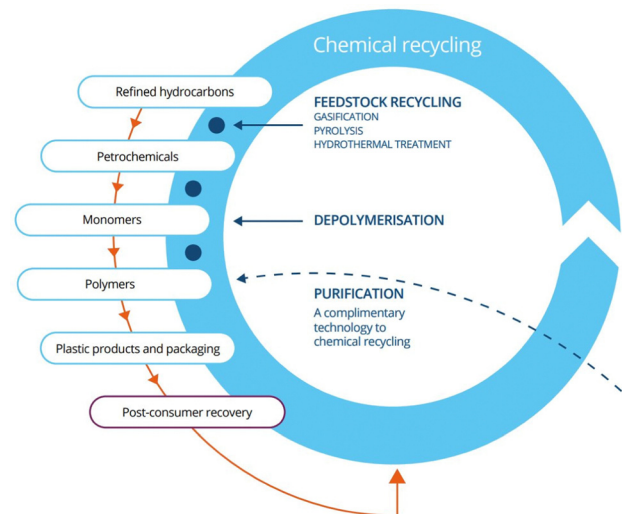


GLOBAL MISMANAGED PLASTIC WASTE GENERATION

Fig. 1 Mismanaged plastic waste trend for three possible scenarios.<sup>3</sup>

undertaking of climate change mitigation efforts.<sup>1</sup> Notably, plastic production and utilisation is becoming more prominent in daily life, as it is a material that is utilized in a huge amount of different day-to-day products, increasing plastic pollution, which demands effective and comprehensive solutions. The trend of mismanaged plastic waste is shown in Fig. 1.<sup>2,3</sup>

Many of these plastic products are designed for single-use, often discarded when they are still in pristine condition.<sup>2,3</sup> In the EU for instance, in 2020, 29.5 million tonnes of post-consumer waste (PCW) plastics were collected and only 10% was sent to recycling plants, the majority of which *via* mechanical recycling.<sup>4–6</sup> This presents a significant challenge, as most of the plastic waste is either consigned to landfills or incinerated. There is considerable potential for expanding thermochemical recycling processes, with pyrolysis emerging as the most notable option.<sup>5</sup> Furthermore, the degradation and depolymerisation of plastic through weathering process leads to the production of micro and nano-plastics. These particles are ingested by animals, thereby being introduced into the food

Fig. 2 Closed loop life cycle of plastic.<sup>11</sup>

chain, and cause food contamination for both animals and humans.<sup>7</sup>

Fast pyrolysis is a thermochemical process that occurs in an inert environment, in the range of 450 to 600 °C and can be used for chemical recycling of biomass or plastic.<sup>8</sup> This process products are separated into three categories: gas, wax, and oil. The resulting pyrolysis oil is a complex mixture composed of acids, alcohols, aldehydes, esters, ketones, sugars, phenols, guaiacols, syringols, furans, lignin-derived phenols, and extractable terpene with multi-functional groups.<sup>9</sup> This is a product that potentially can be utilized as a biofuel, an alternative to petroleum-based fuels, or as feedstock for the chemical industry, which could help the creation of a circular economy<sup>10</sup> (Fig. 2).

Pyrolysis oil, however, usually has a high viscosity, low-density, low pH, high-water content (as high as 15–30 wt%),<sup>9</sup> high oxygen-to-carbon (O:C) ratio and low hydrogen-to-carbon (H:C) content.<sup>12</sup> All these factors make the storage, transport, and utilization of the product more difficult, due to corrosion and instability, as well as lower high heating values (HHV).<sup>8</sup> For effective and widespread usage, the pyrolysis oil needs to be upgraded.<sup>13</sup>



Dr Joy Sumner is a Reader in Energy Materials and Head of the Centre for Energy Engineering at Cranfield University. Dr Joy Sumner's work is related to the degradation mechanisms of materials used in components, most often in energy systems. Her main focus is the mechanisms of failure for steels and nickel-based alloys in simulated real world environments. To achieve this, Joy is involved in several projects including recently the EPSRC-funded "Investigating Corrosion in Supercritical Fluids", and the Innovate UK funded "Plastic Recycling Technology and Outputs: Enhancing Material Longevity and Product Quality for Commercialisation".

Joy Sumner

© 2024 The Author(s). Published by the Royal Society of Chemistry

## 2 Pyrolysis oil composition

### 2.1 Biomass

Biomass is a renewable organic material that comes from plants and animals; its sources include wood, agricultural crops and waste material, municipal solid waste, animal manure and human sewage. Bio-oil, derived from biomass pyrolysis, is a highly intricate mixture whose composition varies with changes in the feedstock, temperature, pressure, residence time and catalysts. Other factors that can lead to different results are pre- and post-treatment of the biomass or the oil.<sup>17</sup> Typical physical-chemical properties of the biomass derived bio-oil are summarized in Table 1.<sup>13</sup>



Table 1 Bio-oil composition matrix and associated ASTM standards<sup>12</sup>

Property (ASTM standard)	Value (average)
C	56 wt%
H	6 wt%
O	38 wt%
N	0.2 wt%
S	0.02 wt%
Water content (D95, E203)	25 wt%
pH acidity (D974, D664, D3339)	2.5
Specific gravity (density compared to water)	1.2
High heating value (D240, D4809)	17 MJ kg <sup>-1</sup>
Viscosity (D88, D445, D2170)	40–100 mPa s
Solids (char content)	0.10 wt%
Density (D1298, D4052)	1.2 kg L <sup>-1</sup>

Pre-treatment is common practice in the industry in which the biomass goes through several physical-chemical processes before being pyrolyzed, such as torrefaction and trituration.<sup>18,19</sup> Pyrolysis oil from a lignocellulosic (*Acacia nilotica*) raw biomass (PO-RAW) and torrefied biomass (PO-TB) are composed of furan derivatives, phenol derivatives, acids, alcohols, aldehydes, ketones, sugar derivatives, esters, and other compounds. Table 2 summarizes the most abundant species.<sup>19</sup>

Temperature is a critical factor during the pyrolysis process, significantly affecting product yields and altering the composition of the resulting oil.<sup>18,20–23</sup> For example, during the pyrolysis of food waste (FW) and food waste solid digestate (FWSD), increasing the temperature from 500 to 800 °C led to a reduction in oil yield, decreasing from 19.5% to 8.2% for FW and from 15.9% to 8.3% for FWSD. Additionally, the yield of aliphatics in the bio-oil decreased from 18.91% to 16.86% for FW and from 33.78% to 25.64% for FWSD. Notably, as the temperature increased, carbon and hydrogen content in the oil increased, while oxygen content decreased. This desirable outcome for improving the oil stability and fuel quality.<sup>22</sup> Rice husk pyrolysis oil composition was also influenced by temperature. Acids concentration varied from 7.07 wt% at 400 °C to 5.69 wt% at 600 °C, although it peaked at 8.46 wt% at 450 °C, ketones presented a similar behaviour, going from 8.65 wt% to 4.14 wt% for the same temperature increase. Aldehydes, phenols and nitrogenated compounds all presented a reduction in the concentration.<sup>23</sup> Using a heavy metal contaminated mangrove as the biomass (temperatures range: 300–700 °C) the main compounds found in all cases were phenol derivatives, carboxylic acids, and alcohols. Analysis by GC-MS showed that independently of the temperature, the most abundant alcohol and phenol derivative were methylpropan-1-ol and catechol, respectively, although concentrations varied. The lower temperature (300 °C) led to a higher concentration of 2-methylpropan-1-ol, catechol, syringol and germanicol. For the higher temperatures (500–700 °C), the most abundant compounds were the same ones. A slight variation of the concentration of 2-methylpropan-1-ol and syringol occurred (0.59 and 0.76% variation, respectively), for catechol and germanicol, the lower temperature resulted in a noticeably higher concentration (2.80 and 2.09% variation, respectively).<sup>24</sup>

Table 2 Chemical composition of pyrolysis oil identified by GC-MS analysis at the optimum conditions of pyrolysis of raw and TB<sup>19</sup>

Compound	Relative content (peak area (%))	
	PO-TB	PO-RAW
<b>Furan derivatives</b>		
2-Furancarboxaldehyde	10.46	—
2-Furanmethanol	5.62	6.05
2(3H)-Furanone, 5-methyl	3.52	5.02
2-Furancarboxaldehyde,-5-methyl	—	6.45
<b>Phenol derivatives</b>		
Phenol, 2-methoxy	5.78	—
Phenol, 4-methoxy	—	8.72
Creosol	3.84	6.05
Phenol, 2,6-dimethoxy	9.46	9.11
3,5-Dimethoxy-4-hydroxytoluene	4.63	4.61
Phenol, 2,6-dimethoxy-4-(2-propenyl)	6.68	0.82
<b>Acids</b>		
<i>n</i> -Hexadecanoic acid	0.60	0.54
Linoelaidic acid	—	1.90
<b>Alcohols</b>		
1-Penten-3-ol	0.80	0.65
1,2-Benzenediol,3-methyl	—	2.15
1-Octen-3-ol,acetate	0.82	—
<b>Aldehydes</b>		
Benzaldehyde, 4-hydroxy-3-methoxy	—	0.8
Benzaldehyde, 4-hydroxy-3,5-dimethoxy	0.64	0.64
<b>Ketones</b>		
Alpha, beta-crotonolactone	2.16	2.16
3-Methylcyclopentane-1,2-dione	2.86	3.93
6-Methoxycoumaran-7-ol-3-one	3.61	—
<b>Sugar derivatives</b>		
1,4:3,6-Dianhydro-alpha-D-glucopyranose	0.30	1.47
Beta-D-glucopyranose, 1,6-anhydro	—	6.39
<b>Esters</b>		
2-(Acetoxy) ethyl acetate	0.53	—
Diethyl phthalate	—	0.55
Di- <i>n</i> -octyl phthalate	0.35	0.31
<b>Other compounds</b>		
1 <i>H</i> -Pyrazole, 3,5-dimethyl	—	9.34
Benzene, 1,2,3-trimethoxy-5-methyl	3.18	1.91

Phenol derivatives, lignin derivatives, benzene derivatives, alcohols and carboxylic acids are the main components of bio-oil, and account for the high oxygen concentration and instability of the oil due to low pH, when compared to conventional oils.<sup>19,24–27</sup> The viscosity is also highly dependent on the feedstock, as reported by Luo *et al.*<sup>25</sup> when comparing lignocellulosic biomass fast pyrolysis bio-oils. The results of the characterization show a total phenolic, lignin derivative and benzene derivative compound content of 32.26%, 32.36%, 15.78% respectively. All main compounds reported are oxygenated, most of which are aromatics. The results are summarized in Table 3.

Due to its highly complex nature, it is common to separate the bio-oil into hydrophilic, also referred to as water soluble bio-oil (WSBO) and hydrophobic shares. This process can increase the number of quantifiable compounds in the



**Table 3** Relative content of main compounds in the organic composition of bio-oil produced from *P. indicus*<sup>25</sup>

Compound	Relative content (%)
Furfural	9.06
Acetoxacetone, 1-hydroxyl	1.21
Furfural, 5-methyl	1.82
Phenol	2.55
2-Cyclopentane-1-one, 3-methyl	1.58
Benzaldehyde, 2-hydroxyl	2.70
Phenol, 2-methyl	5.04
Phenol, 4-methyl	0.51
Phenol, 2-methoxyl	0.27
Phenol, 2,4-dimethyl	9.62
Phenol, 4-ethyl	2.18
Phenol, 2-methoxy-5-methyl	4.15
Phenol, 2-methoxy-4-methyl	0.55
Benzene, 1,2,4-trimethoxyl	3.80
Phenol, 2,6-dimethyl-4-(1-propenyl)	4.25
1,2-Benzenedicarboxylic acid, diisoctyl ester	1.80
2-Furanone	5.70
Levoglucosan	6.75
Phenol, 2,6-dimethoxy-4-propenyl	3.14
Furanone, 5-methyl	0.49
Acetophenone, 1-(4-hydroxy-3-methoxy)	2.94
Vanillin	6.35
Benzaldehyde, 3,5-dimethyl-4-hydroxyl	4.54
Cinnamic aldehyde, 3,5-demethoxy-4-hydroxyl	2.19

analysis, although it remains difficult to identify all components.<sup>26,27</sup> Naturally, the water-soluble fraction presents a higher concentration of water, alcohols, and carboxylic acids, due to their polar nature. Sipila *et al.* reported that WSBO from straw, pine and ensyn (hardwood) oils show a high water content (19.9, 11.1 and 23.2% respectively), low pH (3.7, 2.6 and 2.8 respectively), and high carboxylic acid concentration (10.80, 7.30 and 6.20% respectively). Acetic and formic acids were the most significant components and the main reason for the low pH of the oils.<sup>27</sup> When two commercial wood pyrolysis oils (BTG and Amaron) were separated in water-soluble (WS) and hydrophobic (oil), the authors reported only 34 directly quantifiable compounds, and the main components are shown in Table 4.<sup>26</sup>

## 2.2 Plastics

Characterization of plastic pyrolysis oil shows that the composition is highly dependent on the feedstock and other pyrolysis process factors.<sup>17</sup> Dyer *et al.* studied co-pyrolysis of biomass with several types of plastics and reported on the composition of different plastic pyrolysis oils; the results are summarized in Table 5. These results show that PET is one of the main sources of oxygen in plastic waste, both being highly produced plastics

**Table 4** Compounds identified in the pyrolysis oils and WS fractions by GC-MS (wt%)<sup>26</sup>

Compound	BTG oil	Amaron oil	BTG WS	Amaron WS
Glycolaldehyde	5.60	1.0	16.10	2.90
Acetic acid	3.90	5.50	0.40	0.70
Acetol	5.60	5.50	1.30	1.20
Levoglucosan	3.50	3.00	0.20	0.20
Syringaldehyde	0.10	0.10	8.10	6.80

**Table 5** Characteristics of the pyrolysis oil for different plastic wastes

Proximate analysis (wt%)	HDPE	LDPE	PET	PP	PS
Moisture <sup>a</sup>	0.0	0.0	0.0	0.0	0.0
Ash <sup>b</sup>	4.1	0.3	42.7	0.8	1.6
Volatile <sup>c</sup>	98.1	100.0	94.6	100.0	100.0
Fixed carbon <sup>c</sup>	1.9	0.0	5.4	0.0	0.0

Elemental analysis (%)	C <sup>c</sup>	H <sup>c</sup>	O <sup>c</sup>	N <sup>c</sup>
C <sup>c</sup>	82.5	83.3	69.0	81.0
H <sup>c</sup>	13.1	12.6	5.0	11.4
O <sup>c</sup>	1.8	0.7	32.7	0.6
N <sup>c</sup>	0.1	0.1	0.0	0.1

<sup>a</sup> As received. <sup>b</sup> Dry. <sup>c</sup> Dry ash-free (HDPE: high-density polyethylene; LDPE: low-density polyethylene; PET: polyethylene terephthalate; PP: polypropylene; PS: polystyrene).<sup>28</sup>

(10 wt% of total resin production)<sup>4</sup> and having high oxygen composition (32.7%). Although polyolefins (like PE and PP) present a low oxygen concentration, its major role in the plastic production matrix (57 wt% of all resin produced) make it the largest contributor of oxygenated compounds in plastic oil.<sup>28</sup>

Plastic waste pyrolysis oil usually presents a highly aromatic compound share, when compared to bio-oil, in which can be found monoaromatics, diaromatics, naphthenoaromatics and triaromatics (51.3, 7.5, 5.9 and 2.3 wt% respectively). Some of the main components of the aromatic share of the oil are benzene, toluene, ethylbenzene, xylene, and styrene. The detailed composition of the oil can be found in Table 6.<sup>29</sup>

The feedstock variation is the main factor in plastic-oil composition. In a process treating PET as the feedstock, the resulting pyrolysis oil contains a high concentration of benzene derivatives (10.6 wt%), ketones (5.90 wt%) and acids/esters (62.0 wt%). The most abundant compound in PET pyrolysis oil is benzoic acid and its derivatives, constituting 49.9 wt% of the oil.<sup>30</sup> Cit *et al.* found similar results when comparing polyolefins (PP and LDPE) and PET, where PET pyrolysis oil main components were benzoic acid derivatives (benzoic acid = 23.7, 4-methyl-benzoic acid = 1.6, 4-ethylbenzoic acid = 1.3 and 4-acetylbenzoic acid = 10.3 wt%).<sup>31</sup> LDPE pyrolysis oil has a high share of carbon double bonds, as 39% of its composition are aromatic compounds and other unsaturated carbon molecules.<sup>32</sup> A mix of LDPE and HDPE led to naphthalene derivatives as the main components (approximately 24 wt%) in the plastic-oil, followed by *p*-xylene, toluene, naphthalene, benzene, 1-ethyl-4-methyl-benzene, *m*-xylene, 1,2,4-trimethylbenzene, indane, indene and 1-methyl-3H-indene (approximately 19, 14, 9, 6, 3.5, 3, 2, 1.5, 1.5 and 1 wt% respectively).<sup>33</sup> For PS, monoaromatics are the main components, followed by

**Table 6** Detailed composition of the plastic pyrolysis oil. Edited with permission from ref. 29

Component	Composition (wt%)
Paraffins	5.0
Iso-paraffins	8.2
Olefins	12.3
Aromatics	67.1



Table 7 Main components of plastic-oil<sup>35</sup>

Compound	Composition (wt%)
Xylene	8.80
Benzene	5.30
Chlorinated phenols	4.20
Naphthalene derivatives	4.10
Cresols	3.90
Naphthalene	3.70
Cyclopentene	2.90
Toluene	2.70
Benzene derivatives	1.00
Cyclobutane	0.90

polyaromatics and aliphatics (77.62, 12.86 and 0.01 wt% respectively). As expected, the main component is styrene (73.60 wt%), other noticeable compounds being 2,4-diphenyl-1-butene (7.80 wt%), 2,4,6-triphenyl-1-hexene (2.21 wt%),  $\alpha$ -methylstyrene (1.61 wt%), and toluene (1.58 wt%).<sup>34</sup> When conducting a study on the performance of plastic pyrolysis oil as fuel, Kalagaris *et al.* reported on the composition of the oil. The feedstock was a mixture of styrene butadiene, polyester, clay, ethylene-vinyl acetate, rosin, polyethylene, and polypropylene (47, 26, 12, 7, 6, 1 and 1 wt% respectively). The main components of the oil are presented in Table 7.<sup>35</sup>

The addition of different feedstocks may also change the composition of the oil; that is, the oil composition of a PS/PP mixture may not be just the sum of PS and PP oils. Many of the components found in PP pyrolysis oil, such as methylnaphthalene (8.4 wt%), xylene (7.8 wt%) and phenanthrene (7.6 wt%), completely disappeared when the feedstocks were mixed. Fig. 3 shows the oil composition for several different feedstock compositions. The ratio of each plastic in each mixture was 50/50%, and in the last mixture (PS, PP, PE and PET) the ratio was 40/20/20/20%, respectively.<sup>36</sup>

Both temperature and pressure are vital factors in the pyrolysis process. Pyrolysis of LDPE under different conditions (425 °C/1.60 MPa, 450 °C/2.45 MPa and 500 °C/4.31 MPa) led to variation in both the classes of compounds and their concentration. The carbon chain length also changed, significantly reducing at higher temperatures/pressures. Table 8a shows the variation of the macro composition and Table 8b the specific compounds.<sup>37</sup>

The same variation can be observed in the pyrolysis of PS (process conditions: 400 °C/1.14 MPa, 425 °C/1.26 MPa, 450 °C/1.47 MPa, and 500 °C/1.60 MPa). Results are summarized in Table 9.

Long chain alkanes and alkenes are common products in plastic-oil, and the carbon chain lengths can reach as high as 55 carbons (C<sub>55</sub>) when the feedstock is a mixture of PP, LDPE, HDPE and styrene.<sup>14,15</sup> The carbon number range of alkanes (Table 10a) and alkenes (Table 10b) are as follows:

Plastic waste (polyethylene film and mixed polyolefin) pyrolysis oils blended with fossil naphtha led to an even higher carbon number range. For polyethylene film (PE-film), was C<sub>5</sub>–C<sub>55</sub> and for mixed polyolefin (MPO) was C<sub>5</sub>–C<sub>52</sub>. The composition groups of the resulting pyrolysis oils consisted of

paraffins, iso-paraffins,  $\alpha$ -olefins, iso-olefins, diolefins, naphthenes, monoaromatics and naphthenoaromatics.<sup>15</sup> Both oils also present a substantial amount of several halogen and metal contaminants, among which are found Cl, Br, Al, Ca, Cr, Cu, Fe, Li, Na, Ni, Sb, Si, Sr and Zn. Both Cl and Br can be explained from the initial composition of the feedstock, as polyvinyl chloride (PVC) is a common plastic and bromine is an element that is used in fire retardants. Metal contamination can be traced to plastic enhancers, as metals are commonly used as additives.<sup>15</sup> The detailed composition of the plastic-oil and the distribution of paraffins, olefins, naphthenes and aromatics over the light, medium and heavy product fractions of all post-consumer plastic waste pyrolysis oils can be found in Table 11.<sup>16</sup>

### 2.3 Pyrolysis oil comparison

Although both biomass pyrolysis oil (bio-oil) and plastic pyrolysis oil (plastic-oil) share common components such as paraffins, olefins, aromatics, and oxygenated compounds, they exhibit significant differences in their composition. Notably, bio-oil water content is much higher than plastic oil.<sup>8,12,14–16</sup> On the other hand, plastic-oil presents a higher aromatic share, longer carbon chains and various metal contaminants, added during its production as stabilizers and colouring, for example. The presence of long chain alkanes and alkenes in plastic-oil can lead to a heavier and more viscous product and is a factor that will affect the upgradation process, making it slower.<sup>15</sup>

For utilization as biofuel, HHV is a vital factor. Bio-oil has a lacklustre HHV when compared to transportation fuels (bio-oil HHV: 13–19 MJ kg<sup>−1</sup> compared to gasoline: 44–46 MJ kg<sup>−1</sup> or coal: 25–35 MJ kg<sup>−1</sup>). Plastic-oil, on the other hand, presents a high HHV (41–47 MJ kg<sup>−1</sup>).<sup>8</sup>

The main components from both bio and plastic oil are summarized in Fig. 4.

## 3 Upgrading routes

Bio and plastic oils usually present subpar physical-chemical properties when compared to traditional fuels, such as acidity, O:C and H:C ratios and, for bio-oils, low HHV. This means that for its utilization as an alternative fuel, an upgradation process is necessary. The same is true when it comes to recycling, where these products need to be upgraded to be utilized as feedstock for the petrochemical or chemical industries. Several processes for bio-oil upgradation have been the focus of many studies throughout the years.<sup>9,10,13,38–50</sup> The most common method is deoxygenation, which is commonly accomplished through catalytic cracking and hydroprocessing routes such as hydrotreatment and hydrodeoxygenation.<sup>38</sup>

Upgrading routes can be separated into chemical (hydrotreatment, catalytic cracking, hydrocracking, steam reforming, hydrodeoxygenation and hydrogenation) and physical (distillation, supercritical fluid extraction, liquid–liquid extraction, and emulsification) processing. There are several advantages and disadvantages of each upgrading route; some of the



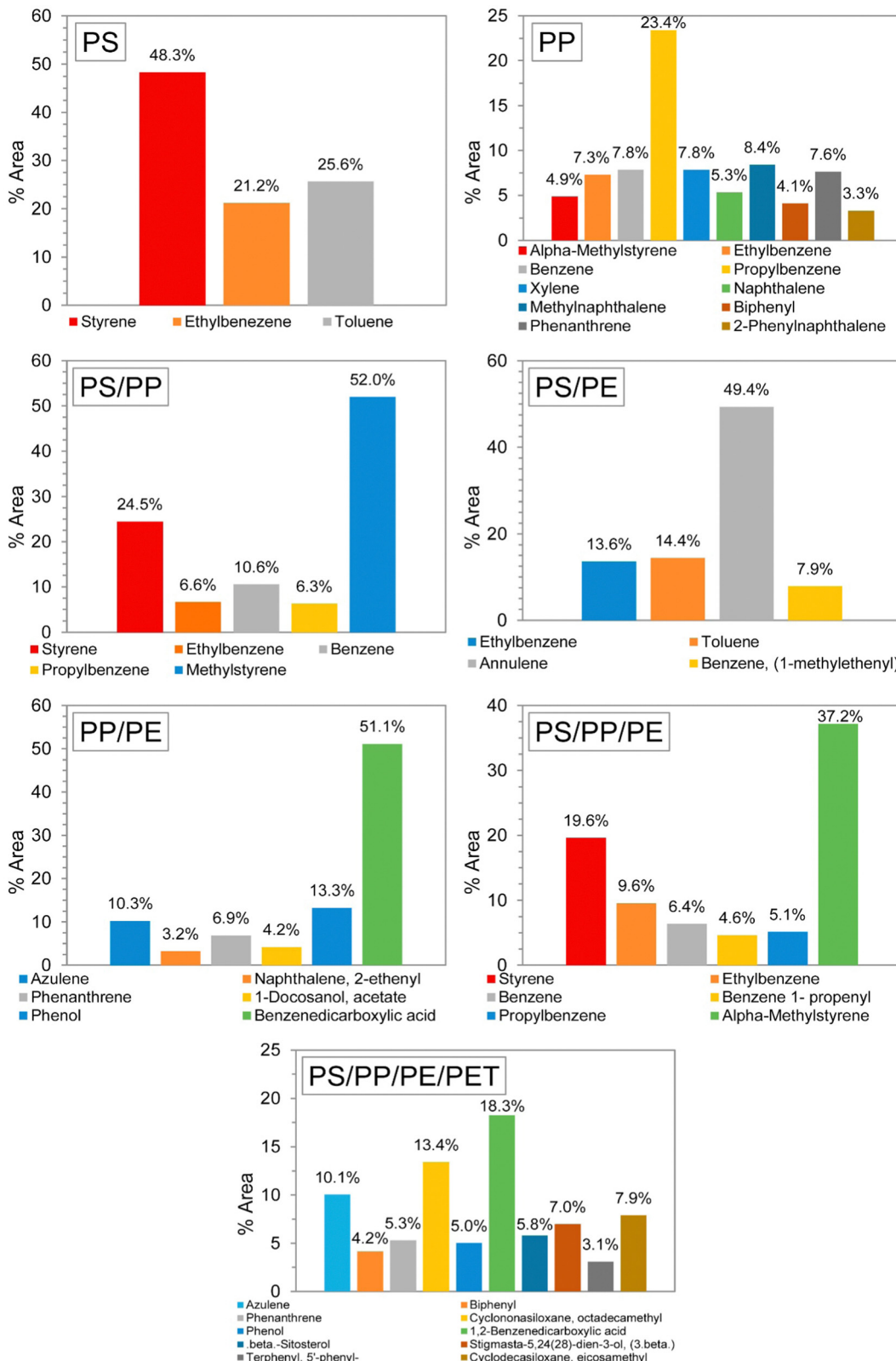


Fig. 3 GC-MS results of liquid oils from pyrolysis of different types of plastic wastes. Reprinted with permission from ref. 36 Copyright 2017 Elsevier.

disadvantages of the more traditional routes are the operational conditions, high costs and coke production. Catalytic cracking is accomplished at medium temperature and atmospheric pressure,

but it leads to catalyst deactivation and the formation of carbon double bonds, which would require further improvement.<sup>51</sup> Decarbonylation and decarboxylation leads to the loss of



**Table 8** (a) Composition of the oil products from the pyrolysis of LDPE (% w/w oil).<sup>37</sup> (b) Main components of the oil products from the pyrolysis of LDPE (% w/w oil)<sup>37</sup>

Composition	425 °C/1.60 MPa	450 °C/2.45 MPa	500 °C/4.31 MPa
<b>(a)</b>			
Naphthenes	2.69	5.56	1.50
Alkanes	46.20	31.7	17.8
Alkenes	12.40	13.1	3.58
Aromatics	12.00	22.9	68.0
Unknowns	19.10	17.9	—
<b>(b)</b>			
Heptane	2.26	3.16	0.46
Toluene	0.35	3.05	24.30
Octane	2.45	3.78	0.19
Ethylbenzene	0.25	0.89	3.06
p/m-Xylene	0.62	1.79	3.90
Allylbenzene	0.21	1.02	4.84
Methylnaphthalene	0.90	0.36	4.22
C <sub>21</sub> –C <sub>30</sub> alkanes	9.98	1.85	1.20

**Table 9** Main components in the pyrolysis oil products from PS (%w/w)<sup>37</sup>

Compound	400 °C/ 1.60 MPa	425 °C/ 2.45 MPa	450 °C/ 4.31 MPa	500 °C/ 4.31 MPa
Benzene	0.38	0.73	1.27	1.63
Toluene	21.70	23.10	27.00	28.40
Ethylbenzene	32.60	39.30	39.00	36.60
Styrene	1.09	0.80	0.39	0.61
Cumene	10.20	9.10	9.36	9.60
Propylbenzene	0.60	0.77	0.90	1.29
Methylstyrene	1.37	0.39	0.33	0.55
Diphenylmethane	0.91	0.83	1.00	1.61
1,2-Diphenylethane	1.44	1.16	0.60	0.37
Phenylnaphthalene	0.98	1.02	1.01	1.25
1,2-Diphenylbenzene	1.27	1.26	1.87	1.89
Triphenylbenzene	6.30	5.13	3.83	3.18

**Table 10** (a) Carbon number range of alkane products of produced pyrolysis oil in wt%. Adapted with permission from ref. 14. (b) Carbon number range of alkene products of produced pyrolysis oil in wt%. Adapted with permission from ref. 14

Feedstock	C <sub>11</sub> –C <sub>20</sub>	C <sub>21</sub> –C <sub>30</sub>	C <sub>31</sub> –C <sub>40</sub>	C <sub>41</sub> –C <sub>50</sub>
<b>(a)</b>				
Polypropylene	2	63	0	0
LDPE	6	54	12	13
HDPE	1	67	18	0
Styrene	0	4	27	8
<b>(b)</b>				
Polypropylene	9.9	8.9	0	0
LDPE	3.3	4.2	0	0.8
HDPE	0.5	6.2	1	1
Styrene	0	0	0	10

valuable carbon. Hydrocracking, hydrodeoxygenation, and hydrogenation require an outside source of H<sub>2</sub>, which is costly and difficult to store (see Fig. 5).<sup>43,44</sup>

### 3.1 Electrochemical hydrogenation

One recently emerging route for pyrolysis oil upgradation is electrochemical processing. Electrochemical hydrogenation

**Table 11** (a) Detailed composition of the plastic pyrolysis oil in wt%. Edited with permission from ref. 15. (b) Detailed composition of the plastic waste pyrolysis oil in wt%<sup>16</sup>

Composition	MPO pyrolysis oil	PE-film pyrolysis oil
Paraffins	32.2	41.9
Iso-paraffins	3.7	3.5
α-Olefins	23.5	33.0
Diolefins	5.3	4.5
Naphthenes	12.4	5.5
Monoaromatics	2.7	1.0
Naphthenoaromatics	0.2	0.1

Composition	Light fraction <sup>a</sup>	Medium fraction <sup>b</sup>	Heavy fraction <sup>c</sup>
Paraffins	28	29	44
Olefins	32	40	29
Naphthenes	18	14	17
Aromatics	19	12	11
Others	4	5	0

<sup>a</sup> Carbon number up to C<sub>20</sub> and boiling point up to 250 °C. <sup>b</sup> Carbon number up to C<sub>30</sub> and boiling point up to 450 °C. <sup>c</sup> Carbon number > C<sub>30</sub> and FBP > 450 °C.<sup>16</sup>

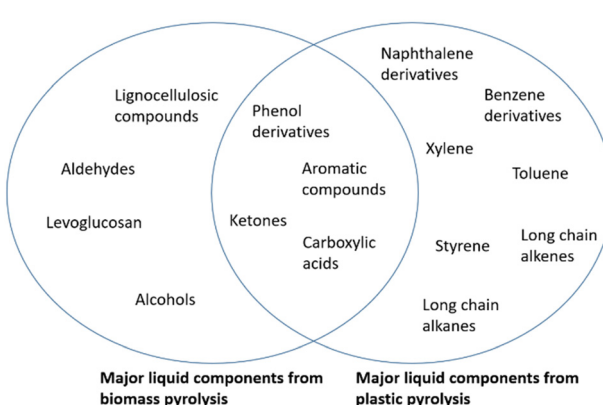
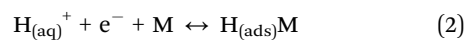
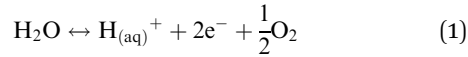


Fig. 4 Intersection in the composition between bio-oil and plastic-oil.

(ECH) does not require H<sub>2</sub> from an outside source, which is produced during the process, reducing costs, and mitigating the risks associated with H<sub>2</sub> storage.<sup>18,39,51</sup> Most setups for ECH consist of two chambers separated by a cathode exchange membrane (CEM). The most prevalent cell design is H-type cells (Fig. 6), although there are some studies utilizing flow type cells.<sup>40,52,53</sup>

During ECH, water is oxidised at the anode (eqn (1)), the resulting H<sup>+</sup>, that can flow through a cation exchange membrane into the cathode cell. The H<sup>+</sup> is then chemisorbed by the catalytic cathode (eqn (2)), where M is the metal surface and H<sub>(ads)</sub>M is the chemisorbed hydrogen.<sup>54,55</sup>



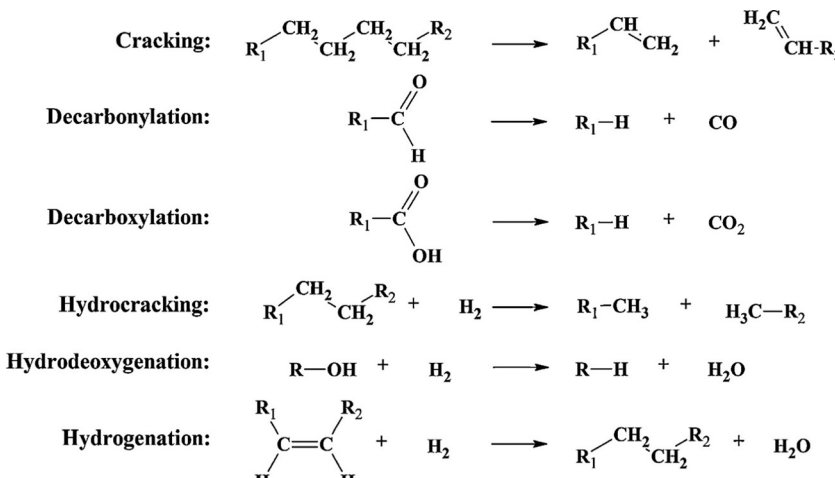


Fig. 5 Examples of reactions associated with catalytic bio-oil upgradation. Reprinted with permission from ref. 44 Copyright 2011 Elsevier Inc.

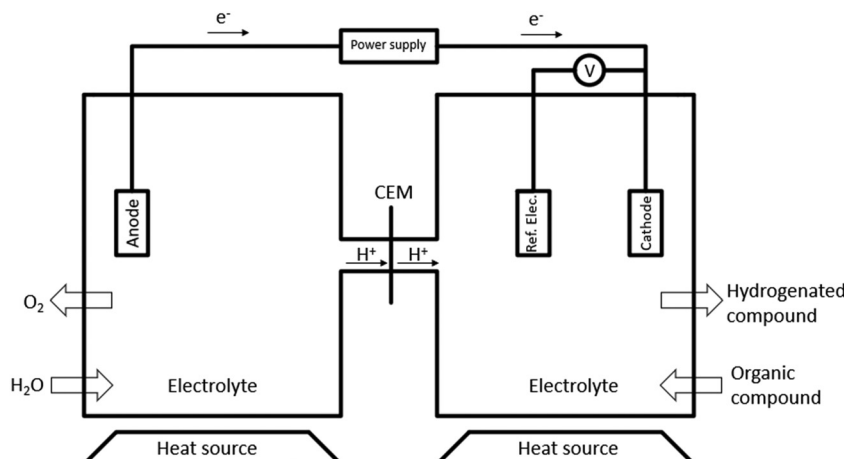
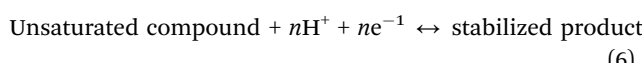
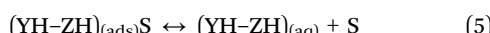
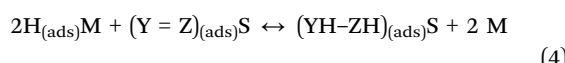
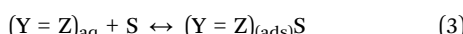


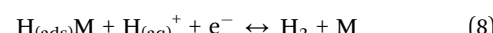
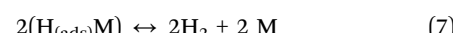
Fig. 6 A typical H-type cell, where the two chambers are separated by a membrane.

In the cathode chamber, the organic unsaturated compound is chemisorbed onto the cathode (eqn (3)), where the hydrogenation process occurs (eqn (4)), followed by the desorption of the stabilized product (eqn (5)). Eqn (6) is the net reaction.<sup>54,55</sup>



where  $(\text{Y} = \text{Z})_{\text{aq}}$  is the unsaturated compound,  $\text{S}$  is the absorption site of the cathode,  $(\text{Y} = \text{Z})_{(\text{ads})}\text{S}$  is the adsorbed organic compound,  $(\text{YH-ZH})_{(\text{ads})}$  is the hydrogenated product before desorption,  $(\text{YH-ZH})_{(\text{aq})}$  is the final product and  $n$  denotes any arbitrary numerical value.<sup>54,55</sup> The hydrogen evolution reaction (HER) is a common side reaction, that can lead to the loss of

hydrogen, rather than reaction with bio-oil, thus reducing the faradaic efficiency (FE), smaller conversion rates, and a poorer overall process. This reaction can occur *via* either the Tafel step (eqn (7)) or the Heyrovsky step (eqn (8)).<sup>54,55</sup>



ECH can be performed under mild conditions ( $< 80^\circ\text{C}$  and 1 atm) (Table 12). Lower temperatures can also avoid catalyst deactivation by coke formation and membrane fouling, potentially reducing the costs associated with catalyst purchase and recycle.<sup>56</sup> However, due to high viscosity and low conductivity, it requires the utilization of membranes, catalysts, and electrolytes to facilitate the reaction.<sup>10,13,38,39</sup> That leads to a vast spectrum of different arrangements that can be organized to optimize the process.

**3.1.1 Key ECH performance parameters.** To understand and quantify the ECH process, the most important parameters



Table 12 Methods for bio-oil upgradation comparison

Method	T (°C)	P (bar)	H <sub>2</sub> need
Cracking	330–700	1.0	No
Hydrocracking	> 400	68–96	Yes
Hydrodeoxygenation	300–600	80–300	Yes
Electrochemical hydrogenation	< 80	≈ 1	No

are faradaic efficiency (eqn (9) and (10)), conversion (eqn (11)), selectivity (eqn (12)) and current density (eqn (13)). Due to difficulties in measuring the surface area of the cathode, and therefore the current density, some authors report this parameter as current (usually in mA), these will be highlighted in the following sections.

$$\text{FE (\%)} = \frac{(I \times T - 2 \times n \times F)}{(I \times T)} \quad (9)$$

where  $I$  = current in A;  $T$  = time in s;  $n$  = moles of hydrogen;  $F$  = Faraday's constant.

This equation can also be simplified:

$$\text{FE (\%)} = \frac{\text{Electrons used to generate products}}{\text{Total electrons passed}} \times 100 \quad (10)$$

$$\text{Conversion (\%)} = \left( \frac{\text{Moles reactant consumed}}{\text{Initial moles reactant}} \right) \times 100 \quad (11)$$

$$\text{Selectivity (\%)} = \left( \frac{\text{Moles desired product}}{\text{Total moles product}} \right) \times 100 \quad (12)$$

$$\text{Current density (mA cm}^{-2}\text{)} = \frac{\text{Current}}{\text{Surface area}} \quad (13)$$

### 3.2 ECH reactor design considerations

**3.2.1 Electrodes.** Electrodes usually consists of conductive materials and catalyst, which play a vital part in the ECH process. Different electrodes can increase bio-oil conversion and interfere with product selectivity.<sup>51</sup> Noble metals,<sup>39,51</sup> base metals,<sup>41,57,58</sup> and graphite,<sup>59</sup> besides catalyst-coated carbon cathodes (*e.g.* Ru/ACC)<sup>39,41,56</sup> have been reported for ECH bio-oil and model compounds upgrading. Pt, Rh, Ru, Au and Pd have been employed as cathode materials during ECH of aldehyde and phenolic model compounds.<sup>51,60,61</sup>

The choice of cathode can greatly interfere with the process, as early transition metals (*e.g.* Ti, Mn, Nb) and platinum group metals (Ru, Rh, Ir, and Pt) have higher affinity toward hydrogen formation, leading to more H<sup>+</sup> in solution, which increases collision probability and, in turn, leads to higher conversion rates.<sup>51</sup> Cathode surface coverage (or adsorption rate) can lead to the same problem of low collision probability, and is dependent on cathode/compound pairing, for example, the adsorption of phenol on Pt is stronger compared to guaiacol.<sup>42,62</sup>

Cathode selection can also influence the selectivity of the process and the desirable product yield. For the ECH of glucose, late transition metals (*e.g.* Fe, Cu, Pd, Ag and Au) led to higher sorbitol formation and post-transition metals (In, Sn,

Sb, Pb, and Bi), Zn and Cd (d metals) favoured d 2-deoxysorbitol formation. Ni had the lowest and Pb the highest sorbitol formation potential.<sup>63</sup>

Platinum group metals (Pt, Pb, Ru, Rh and Ir) are commonly used in hydrogenation processes, due their stability and high affinity towards hydrogen production and have been employed under several conditions and for different compound classes.<sup>63</sup> For the ECH of indigo, a highly unsaturated compound that contains both oxygen and nitrogen (reaction conditions: 1 M NaOH, 50 °C, 20 mA cm<sup>-2</sup>) using RANEY® nickel electrodes doped with different noble metal catalysts (Pt, Pd and Pd/C), Pt coating led to both optimal conversion and FE (10.2 and 8.16% respectively), followed by Pd (8.6, 6.88%), Pd/C (4.7, 3.76%) and RANEY® nickel without coating (4.4, 3.5%).<sup>64</sup> Nobel metals are also capable of hydrogenating phenolic compounds at high conversion rates and FE. ECH of phenol on several cathodes (Pt/C, Rh/C, and Pd/C) demonstrated that Rh/C exhibited the highest hydrogenation rate, the order was Rh/C > Pt/C > Pd/C.<sup>65</sup> Du *et al.* reported on the ECH of phenol on several different electrocatalysts: Pt, Ru, Pt<sub>3</sub>Ru, Pt<sub>3</sub>Sn, Ru<sub>3</sub>Sn, and Pt<sub>3</sub>RuSn supported on carbon cloth (reaction conditions: 0.2 M H<sub>2</sub>SO<sub>4</sub> containing 10 mM phenol at -100 mA, 50 °C for 100 min). Pt<sub>3</sub>Ru/CC presented the highest conversion rate, at 96.3%, followed by Pt<sub>3</sub>RuSn/CC and Pt/CC (91.5 and 90.2% respectively).<sup>66</sup> The concentration of the metal on the surface of the carbon can also lead to different results, although graphite alone was unable to react (reaction conditions: phenol, electrolyte 0.1 mol L<sup>-1</sup> H<sub>2</sub>SO<sub>4</sub> (30 mL), 30 mA, Pt sheet as the anode). 1% Pt/G and 1.5% Pt/G presented the highest conversion rates, both 95%. The highest yield of cyclohexane and the highest FE were 30.4% and 20.3%, respectively, both occurred with the same cathode (1.5% Pt/G). The results are summarized in Table 13.<sup>55</sup> As shown in previous sections, lignin pyrolysis oil can contain phenolic compounds (phenol, *p*-cresol, 4-ethylphenol, and 4-propylphenol, as well as guaiacol) which can be hydrogenated into their corresponding alkylcyclohexanols at high conversion rates using Ru/ACC as the catalytic cathode. The same cathode is effective for transforming model lignin monomers into cyclohexanol.<sup>56</sup>

Metals outside the platinum group can also be utilized as the catalytic cathode, although it still requires more investigation. The ECH of guaiacol and related lignin models utilizing a

Table 13 ECH of phenol on various cathodes<sup>55</sup>

Cathode	Conversion (%)	F.E.	1	2	3	4
Pt	0	0	0	0	0	0
Ni/G	0	0	0	0	0	0
Rh/G	90	0	0	65.7	24.3	0
Pd/G	18	0	0	12.6	5.4	0
0.5% Pt/G	92	11.1	16.6	57	12	5.5
1% Pt/G	95	15.2	22.8	52.3	16.2	3.8
1.5% Pt/G	95	20.3	30.4	58.9	5.7	0
2% Pt/G	90	9.1	13.5	60.3	9	7.2
Graphite	0	0	0	0	0	0

Where [1] is cyclohexane, [2] cyclohexanol, [3] cyclohexanone and [4] benzene.



nickel cathode and a Co/phosphate anode presented high selectivity towards cyclohexanol formation (>99%), with only traces of 2-methoxycyclohexanol. Other experiments were done utilizing cobalt and copper as catalyst cathodes, and only Co formed trace amounts of cyclohexanol and phenol, Cu completely failed in producing these products.<sup>58</sup> The ECH of aldehyde compounds shows that aromatic aldehydes have a higher conversion rate than aliphatic aldehydes. Au, Ag, Cu, and C catalysts exhibit the highest conversion to alcohol products.<sup>67</sup>

**3.2.2 Electrolyte.** Electrolytes can affect the ECH of bio-oil in three major ways. First, the adsorption of anions from the electrolyte into the electrode can make the process difficult. Second, the pH of the solution has a direct relation to product selectivity. Lastly, alcohol has been reported to reduce conversion rate and faradaic efficiency.<sup>42,65,68</sup> The addition of different alcohols (methanol, ethanol, or isopropanol) to the electrolyte led to lower conversion rates and faradaic efficiency as the alcohol concentration increased. Carbon chain length was a factor, as the impact was greater for longer chains.<sup>68</sup>

Electrolytes are needed during ECH to increase the conductivity of the system, although they can interfere with the process. Acids, alkalis, and salts can achieve these results, and the selection of electrolytes should take into consideration both the organic compound and the cathode. Another challenge during this selection is that the electrolyte that presents the highest conversion rate and the one that leads to the highest FE might not be the same one. For the ECH of guaiacol (reaction conditions: 3-CE-NH<sub>3</sub> cathode, 80 °C and 100 mA), the conversion rates, FE and product selectivity varied greatly. The highest conversion rates were NaOH (62 ± 2.4%), NaCl (64 ± 8.8%), and HCl (75 ± 3.9%). For FE, the order was NaCl (20 ± 2.2%) < NaOH (28 ± 1.0%) < HCl (30 ± 4.3%). Similar results were reported for phenol and syringol.<sup>39</sup> The pH of the system can interfere with the results, as demonstrated by the ECH of guaiacol where HClO<sub>4</sub> as the electrolyte led to the highest guaiacol conversion rates, HCl and H<sub>2</sub>SO<sub>4</sub> led to moderate conversion rates (PtNiB/CMK-3 cathode, 0.2 M HClO<sub>4</sub>, 0.2 M HCl and 0.2 M H<sub>2</sub>SO<sub>4</sub> as electrolytes). In addition, HClO<sub>4</sub> achieved optimal selectivity for the desirable product (KA oil). However, increasing the concentration of sulfuric acid from 0.2 M to 0.5 M reduced the ECH activity.<sup>42</sup>

Different catholyte/anolyte pairings can also lead to vastly different results. Acid/acid pair (catholyte/anolyte respectively) lead to higher guaiacol conversion. (Conditions:  $T = 50$  °C,  $I = 300$  mA ( $j = -109$  mA cm<sup>-2</sup>), catalyst = 5 wt% Pt/C (0.133 g), reaction time = 2 h, concentration of all electrolytes = 0.2 M) followed by salt/acid and acid/alkali. Alkali/acid completely failed in generating products. ECH of phenol led to similar results.<sup>62</sup>

**3.2.3 Temperature.** Temperature is a factor that can greatly influence the results of ECH. FE, conversion rates and product selectivity have been reported to be affected by temperature.<sup>39,51,69</sup> Lower temperatures favours electrocatalytic hydrogenation, whilst high system temperature is favourable for hydrogen desorption, which leads to the low ECH performance.

This condition increases the water oxidation rate on the anode, which contributes to hydrogen evolution reaction (HER), a competing reaction, due to H<sup>+</sup> generation and transfer to the cathode.<sup>51</sup> For the ECH of indigo, increasing the temperature from 30 to 60–80 °C led to an FE increase, although it substantially dropped down at higher values. Optimal reported temperature was 70 °C.<sup>64</sup> Guaiacol (HCl as catholyte,  $T = 2$  h, 100 mA) behaves in a similar way, where raising the temperature from 25 °C to 50 °C increased FE from 8% to 17% but further increase to 80 °C dropped it back to 10%.<sup>39</sup> Increasing temperature from 5 to 40 °C during phenol to cyclohexanol ECH upgrading significantly increased FE, upon further heating to 60 °C, FE increase was continuous, but minimal.<sup>70</sup>

**3.2.4 Current and potential.** Current density can have a direct impact on product selection, FE, and conversion rates, as it can lead to higher H<sub>ads</sub> desorption from the cathode and thus become an obstacle for the main reaction.<sup>51,54,55</sup> Although higher current densities could decrease the overall process quality, insufficient current can do the same as insufficient current can lead to a lower concentration of H<sub>ads</sub> on the cathode surface. This reduces collision probability and, consequently, reduces FE.<sup>51</sup> Current is directly linked to potential values, and therefore can also interfere in the reaction pathways and product selectivity. The major side reaction that can occur during the ECH process is the Hydrogen Evolution Reaction (HER), which leads to lower FE and product yield. The HER usually occurs by Tafel or Heyrovsky reactions (eqn (7) and (8)).<sup>51,57</sup> The surface coverage of H<sub>ads</sub> is determined by the kinetics of eqn (2) and side reactions, eqn (7) and (8), which can be increased or decreased depending on potential. Therefore, potential is an essential factor of the ECH process.<sup>54,57</sup> For the ECH upgrading of phenol, an increase on current from the range of 10–30 to 30–70 mA slightly lowered product yields and FE. Further increase on the current to over 70 mA highly decreased the overall process quality.<sup>55</sup> Furfural behaves in a similar way (desirable product: furfuryl alcohol and 2-methylfuran) where the increase of current density from 300 to 1200 mA dm<sup>-2</sup> led to a decrease in FE.<sup>54</sup> Current density increase during the ECH of lactic acid to lactaldehyde and propylene glycol (0.01 M H<sub>2</sub>SO<sub>4</sub> for 9 h at 90 °C) led to a lower product yield<sup>71</sup> (Tables 14 and 15).

## 4 ECH systems for model compound and bio-oil upgradation

### 4.1 Model compounds

Zhou *et al.* proposed a new catalyst for electrocatalytic hydrogenation (ECH) of guaiacol, a boron-doped PtNiB/ordered mesoporous carbon (CMK-3) cathode on a Nafion 117 membrane and IrO<sub>2</sub>/C as the anode. The goal was the production of KA oil (a mixture of cyclohexanol and cyclohexanone) which is highly utilized as industrial feedstock.<sup>42</sup> The working temperature was 60 °C. The anolyte was 10 mL 0.2 M HClO<sub>4</sub> and catholyte was 10 mL 0.2 M HClO<sub>4</sub> with 10 mM guaiacol.



Table 14 Previous studies comparison table

Cathode	Feedstock	Conversion	Electrolyte	Temperature (°C)	$J$ (mA cm $^{-2}$ )	F.E.	Duration (h)	Ref.
Ru/ACC	Guaiacol	64 ± 8.8	NaCl	80	100 <sup>a</sup>	20 ± 2.2	2	39
	Phenol	75 ± 3.9	HCl			30 ± 4.3		
	Syringol	89	HCl			29		
PtNiB/CMK-3	Guaiacol	58	HCl	60	20 <sup>a</sup>	29	2	42
	Guaiacol	>99%	HClO <sub>4</sub>			86.2		
	Phenol	>99%	BK <sub>3</sub> O <sub>3</sub>			8	6	58
RANEY <sup>®</sup> -Ni	Guaiacol	100	HCl	75	100 <sup>a</sup>	26		
	4-Methylphenol	100	HCl			20	4	56
	4-Ethylphenol	98	HCl			9		
RANEY <sup>®</sup> -Ni	4-Propylphenol	100	HCl	80	100 <sup>a</sup>	6	6	64
	Indigo	4.4	NaOH			3.5		
	4.4	10.2	NaOH			8.16		
RANEY <sup>®</sup> -Ni with Pt	8.6	8.6	NaOH	50	20	6.88	—	—
	4.7	4.7	NaOH			3.76		
	Furfural	97 ± 1.4	NH <sub>4</sub> Cl			6	5	54
Iron		90.2		—	29 ± 3.5	34.6	5	54
Pt/CC		73.4				28.2		
Ru/CC		96.3	H <sub>2</sub> SO <sub>4</sub>			37.6	1.67	66
Pt <sub>3</sub> Ru/CC	Phenol	73.3	H <sub>2</sub> SO <sub>4</sub>	50	100 <sup>a</sup>	29.7		
Pt <sub>3</sub> Sn/CC		62.3				26.7		
Ru <sub>3</sub> Sn/CC		91.5				39.5		
Pt <sub>3</sub> RuSn/CC								

<sup>a</sup> Reported as mA.

Table 15 Different setups and studies comparison table

Feedstock	Cathode	Catholyte	Anode	Anolyte	$T$ (°C)	Duration (h)	$J$ (mA cm $^{-2}$ )	Ref.
Guaiacol	Boron-doped PtNiB/ordered mesoporous carbon (CMK-3)	0.2 M HClO <sub>4</sub>	IrO <sub>2</sub> /C	0.2 M HClO <sub>4</sub>	60	5	40 <sup>a</sup>	42
Phenol derivatives	Ru/ACC	0.2 M HCl	Pt wire	0.2 M phosphate	80	—	100 <sup>a</sup>	56
WSBO	Ru/ACC	0.2 M NaCl	Pt wire	1 M H <sub>2</sub> SO <sub>4</sub>	27	6.5	480 <sup>a</sup>	72
WSBO	Ru nanoparticles on mesoporous carbon–Ru@OMC	WSBO	Fe(III)/Fe(II) + carbon felt	Wastewater or lignin	—	3	—	41
Resin wood (ponderosa pine) bio-oil	Metal-free (carbon)	1 M Na <sub>2</sub> SO <sub>4</sub>	Ti sheets/ Pt coating	Purified water	35(±2)	—	—	40

<sup>a</sup> Reported as mA.

The flow rate was 50 mL min $^{-1}$ . Constant current of 20 mA for 2 h. The setup is shown in Fig. 7.<sup>42</sup>

Faradaic efficiency (FE) of the process was 86.2%, in comparison to the 6.3% that was found when the reaction was carried out in a PtNi/CMK-3 cathode, that is, without boron doping. The conversion rate was respectively <99.0% and 11.7%. The study also reported on the ECH of other phenolic compounds using PtNiB/CMK-3. All achieved high (<95%) conversion rates and high (<80%) FE. The temperature increase effect on conversion rate and FE on range of 20–60 °C was positive (conversion rate: from 58% to 98.9% and FE: from 45% to 86.2%), but further heating to 80 °C reduced these parameters to 78% and 57% respectively<sup>42</sup> (Fig. 8).

Garedew *et al.* studied the ECH of phenolic compounds. Several model compounds were selected, including catechol, anisole, phenol, guaiacol, 3-methoxyphenol, 4-methoxyphenol, syringol, 1,3-dimethoxybenzene, *o*-cresol, *m*-cresol, *p*-cresol, creosol, vanillin, syringaldehyde, eugenol, 4-ethylphenol, 4-propylphenol, 4-propylguaiacol and 4-ethylguaiacol.<sup>56</sup>

The cell setup was a H cell, separated by a Nafion 117 membrane. The cathode was Ru/ACC and the anode a Pt wire. Catholyte was a 0.2 M HCl solution (30 mL) and the anolyte a 0.2 M phosphate buffer (30 mL). Temperature was maintained at 80 °C and the experiment was run at 100 mA. The cell setup is shown on Fig. 9.<sup>56</sup>

The authors reported that increasing guaiacol concentration from 5 to 20 mM increased the FE and product selectivity. Further increases from 20 to 60 mM had led to a steep decline in the conversion rate, although this was mitigated by increasing the duration of the process (Fig. 10).

Phenol, *p*-cresol, 4-ethylphenol, and 4-propylphenol, as well as guaiacol, were transformed into their corresponding alkyl-cyclohexanols at high conversion rates (>98%). Carbon chain length was a determinant factor in reaction speed, as increased lengths resulted in slower conversions.<sup>56</sup>

#### 4.2 Water soluble bio-oil (WSBO)

Li *et al.* proposed ruthenium (Ru) supported on activated carbon cloth (ACC) as the catalytic cathode as the electrocatalyst.



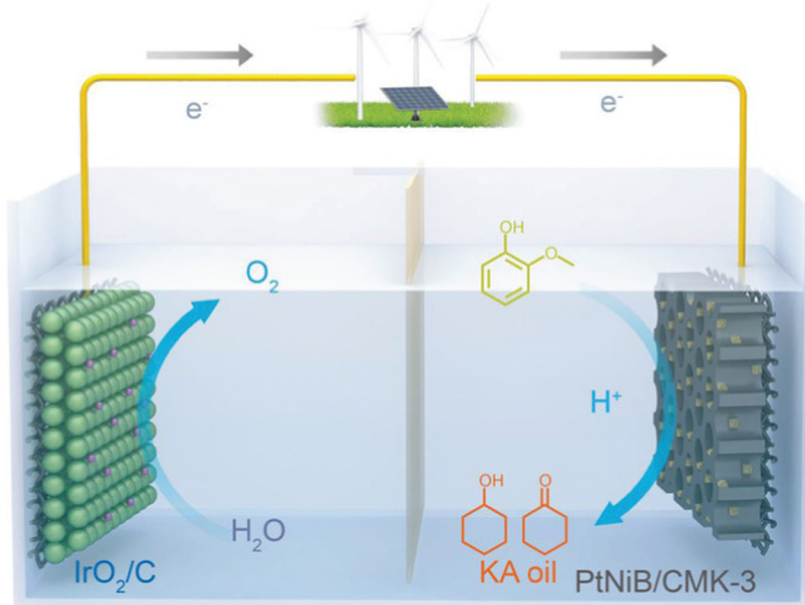


Fig. 7 Schematic of ECH of guaiacol into KA oil integrated with  $O_2$  production, equipped with PtNiB/CMK-3 and  $IrO_2/C$  as the cathode and anode, respectively. Reprinted with permission from ref. 42 Copyright 2019 Wiley.

The bio-oil was mixed with water, in water to bio-oil ratio of 4 : 1, with bio-oil final concentration of 15 wt%. The mixture was then centrifuged, and the top layer was separated as the water-soluble bio-oil (WSBO).<sup>72</sup> The same group has proved that this cathode was capable of hydrogenating guaiacol, syringol and phenol, as showed in the previous sessions.<sup>39</sup>

Electrochemical hydrogenation of WSBO was carried out in a two-chamber glass H-cell, separated with a DuPont<sup>®</sup> Nafion117 membrane (see Fig. 11). The reaction temperature was 27 °C and the pressure was 1 atm. Anolyte consisted of 1 M sulfuric acid and Pt wire was used as the anode. A mixture of WSBO with 0.2 M NaCl served as the catholyte. Current was 480 mA.<sup>72</sup>

After the 6.5 h treatment, most of the organic compounds were depleted or fully converted by hydrogenation, the proposed mechanisms are shown in Fig. 12. Removal of >50% of acetic acid is an expressive result, as it is a major contributor to bio-oil corrosiveness. No coke formation was observed. The same experiments were done using only ACC as the cathode and showed that Ru is an essential part of the proposed ECH process.<sup>39</sup>

Although a noble metal catalyst (e.g., Pt and Ir) as the anode is normally used to ensure effective water oxidation, Zhang *et al.* found that a Fe(III)/Fe(II) redox pair can be utilized as a substitute when combined with carbon felt as the anode. This change can make the process less expensive and can further its usage. The authors presented a Ru-based ECH cathode catalyst by uniformly embedding Ru nanoparticles into the surface of the ordered mesoporous carbon (OMC) support (noted as Ru@OMC). The catholyte solution was WSBO, duration was 3 h.<sup>41</sup> The cell setup is shown in Fig. 13.

The EHC treatment led to an increase in the H:C ratio and a decrease in the O:C ratio. Another result was the content

reduction in several organic groups, such as acids, esters, carbonyls, phenols, sugars, and furans. The alcohol content increase was substantial, and the process elevated the selectivity of polyhydric alcohols. The results infer that this technique provides de ability to saturate unsaturated components in WSBO.<sup>41</sup>

#### 4.3 Whole oil

Lister *et al.* employed both an anion exchange membrane (AEM) and a cation exchange membrane (CEM), in what is described as a dual exchange membrane (DEM) to upgrade a whole pyrolysis bio-oil mixed with an aqueous phase containing acetic acid and formic acid. The concentrate vessel was filled with 10 mL solution of 1 M  $Na_2SO_4$ . The oil was filtered to remove any char particles, a common product from pyrolysis. Fig. 14 shows a diagram of the electrolysis system used in this work.<sup>40</sup>

The cell temperature was held at 35 °C ( $\pm 2$  °C), the fluids flow rate was 2 mL min<sup>-1</sup>. A metal-free carbon catalytic cathode was chosen to prevent hydrogen evolution reaction (HER). The process achieved an increase in the pH from 2.6 to >4 and a significant reduction in total acid number (TAN). There were no signs of coke formation, improving carbon efficiency and catalyst lifetime. Although membrane degradation was noticed.<sup>40</sup>

## 5 Outlook of previous studies

The electrochemical approach to upgrading bio-oils is a technique that can be performed at mild temperatures (<80 °C) and pressure (1 atm). This is an essential condition for a



Entry	Structural formula	t (min)	Conv. (%)	FE (%)	Product (sel. %)
1		50	97.5	90.8	 89.8 10.1
2		60	95.8	92.6	 60.6 39.3
3		60	95.1	88.1	 60.7 34.4
4		90	98.7	84.3	 85.9 12.1
5		90	97.5	86.2	 83.5  16.1
6		90	98.6	80.2	 81.6 11.8

Fig. 8 ECH of other phenolic compounds using PtNiB/CMK-3. Reprinted with permission from ref. 42 Copyright 2019 Wiley.

cheaper product, as traditional methods are energy intensive. Also, in thermal stabilization and deoxygenation, oxygen is released as  $\text{CO}_2$ ,  $\text{CO}$ , and  $\text{H}_2\text{O}$ . These products represent a loss of expensive carbon and  $\text{H}_2$ .<sup>40</sup> The research gap that exists is on what are the ideal catalysts, membranes, cell configuration and how to increase the oil's low conductivity. Understanding the mechanism of the reaction and the behaviour of the compounds is a key part of the process, so model compound studies are necessary. Another way of simplifying the process so it can

be more easily studied is utilizing WSBO as a feedstock; this allows the study to circumvent the challenges brought by the complexity of a mixture that contains both polar and non-polar compounds. Most studies have focused on either model compounds or WSBO, and therefore ECH of whole pyrolysis oil still needs further investigation. Zhenglong *et al.* demonstrated that the separation of WSBO can lead to a higher organic compound conversion. Ruthenium was used as the basis for the catalyst cathode, this metal was also utilized by Zhang *et al.*, Zhou *et al.*



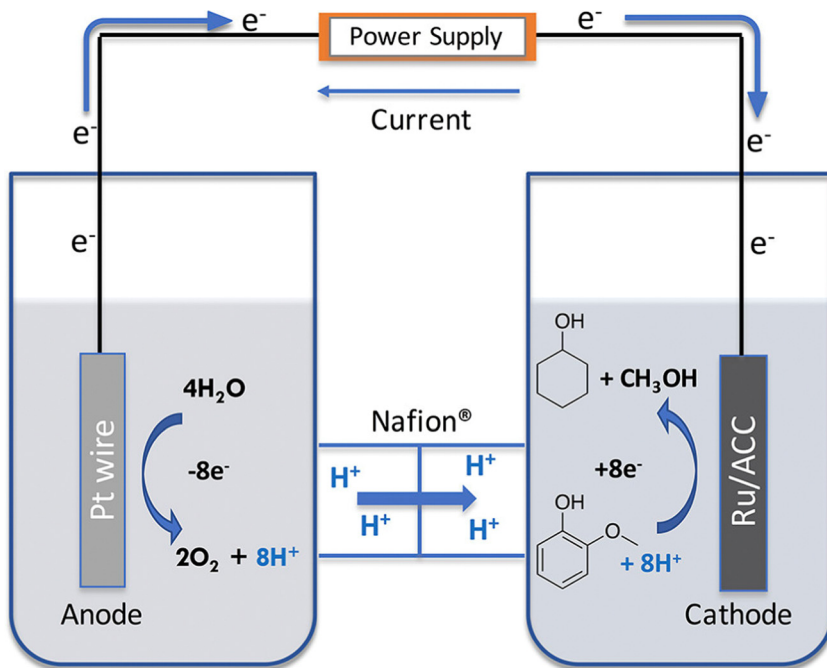


Fig. 9 Electrocatalytic hydrogenation in a two-chambered H cell. Reprinted with permission from ref. 56. Copyright 2019 American Chemical Society.

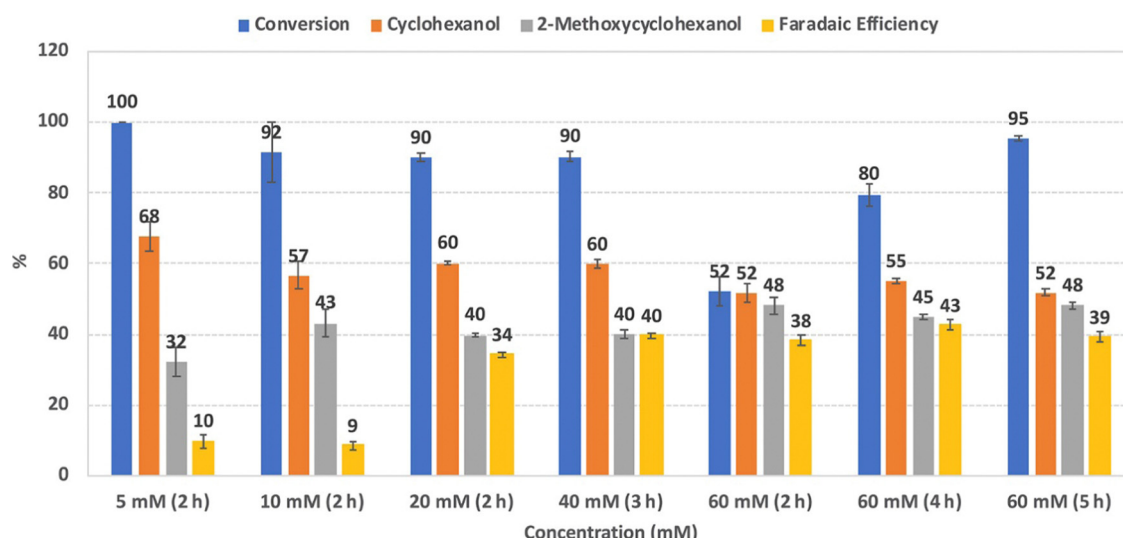


Fig. 10 Conversion, product selectivity, and faradaic efficiency of guaiacol reduction using different substrate concentrations (5, 10, 20, 40, and 60 mM) at 100 mA and 80 °C. Error bars are standard error. Reprinted with permission from ref. 56. Copyright 2019 American Chemical Society.

and Gardew *et al.* The authors also proposed reactions for some compounds (see Fig. 12), this shows that hydroxyl groups, such as ketones, carboxylic acids and alcohols are resistant to hydrogenation, whereas double bonds were almost depleted. Gardew *et al.* also reported that, for phenolic compounds, the double bonds inside the aromatic ring were hydrogenated, when the hydroxyl group was not (e.g., phenol was converted into cyclohexanol and cyclohexanone rather than benzene). These data were extrapolated for the main components in plastic pyrolysis oil (see Fig. 15). It is worth noting that,

although cyclohexane is a possible product of phenol hydrogenation, the process of C–O cleavage, which would involve the hydrogenation of cyclohexanol into cyclohexene ( $C_6H_{12}O \rightarrow C_6H_{10}$ ), followed by cyclohexene into cyclohexane ( $C_6H_{10} \rightarrow C_6H_{12}$ ) would require much higher temperatures and overpotentials.<sup>62</sup>

Carbon loss during the ECH process was reported by Zhenglong *et al.*, as only 80% of the carbon was retained in the cathode chamber. 6.0% was found in the anode chamber, due to migration through the membrane, 2.6% was adsorbed by the

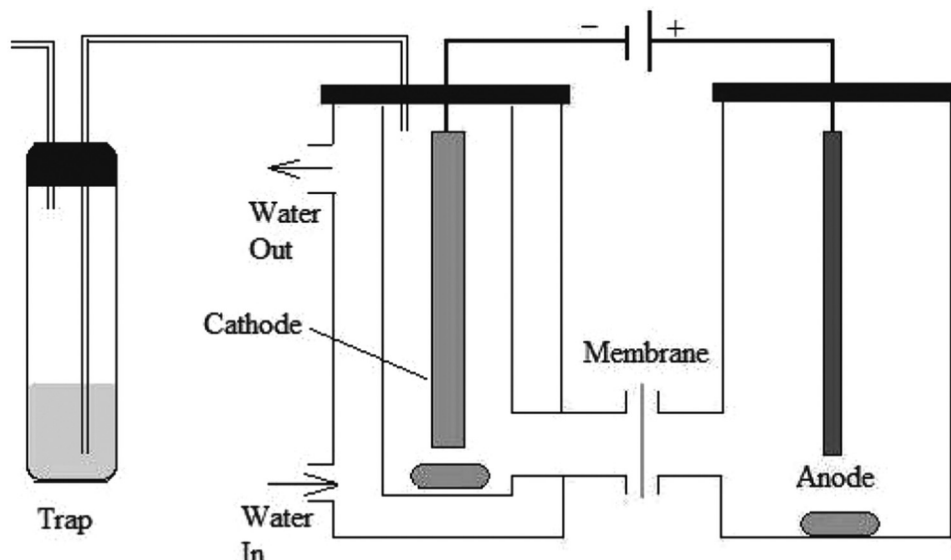


Fig. 11 Electrochemical hydrogenation cell setup for ECH of water-soluble bio-oil.<sup>72</sup>

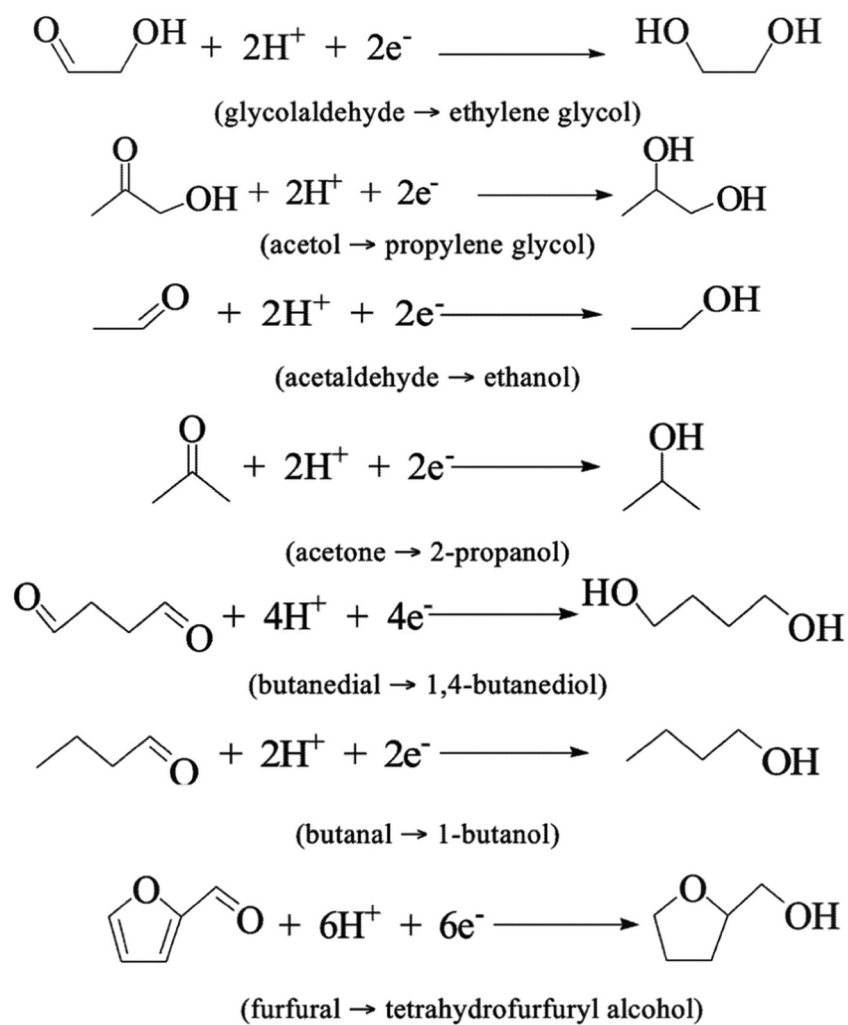


Fig. 12 Reductions via ECH of organic compounds in water-soluble bio-oil.<sup>72</sup>

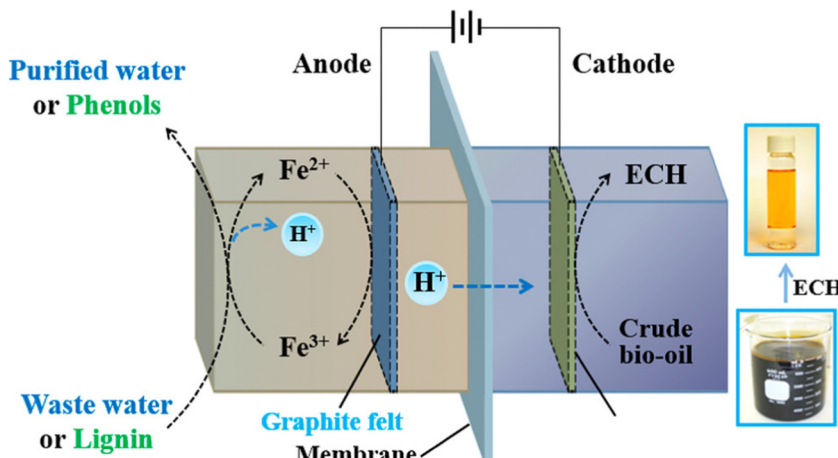


Fig. 13 Schematic illustration of low-energy ECH of bio-oil: experimental setup. Reprinted with permission from ref. 41. Copyright 2018 American Chemical Society.

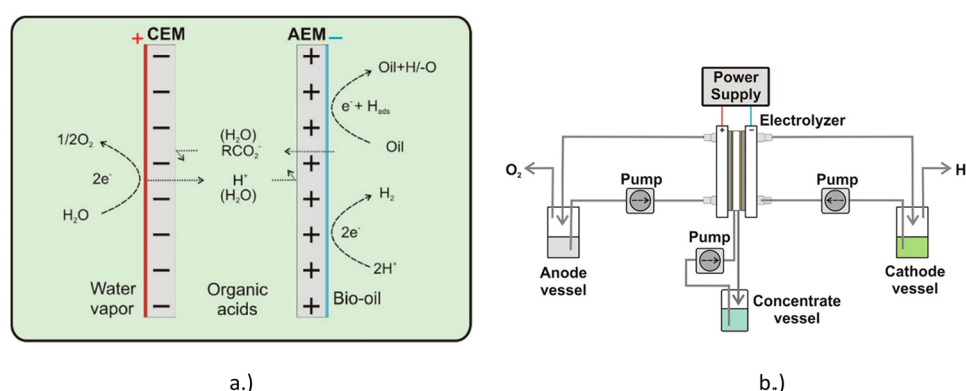


Fig. 14 Spatial chemical representation (a) and diagram of the separation–hydrogenation process (b). Reprinted with permission from ref. 40. Copyright 2018 American Chemical Society.

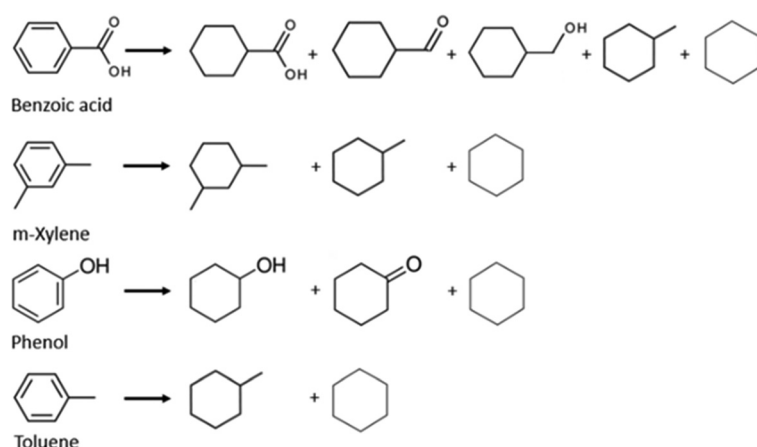


Fig. 15 Main components from plastic pyrolysis oil and the possible products from ECH.

cathode and 0.2% was trapped in the downstream water trapping system. The system's total carbon loss was 11.2%. The

authors suggest that the rest could be inside the membrane, as it turned black after the process.<sup>72</sup> This exemplifies how

different membranes could lead to a better result, as the carbon loss could possibly be avoided. Also, the process cost is increased by constantly changing the system's components. Zhang *et al.* showed that a cheaper anode, the Fe(II)/Fe(III) redox pair, can be utilized as a substitute for the commonly used noble metal (*e.g.* Pt) as a way to make the overall process cheaper and more competitive.

The work of Zhou *et al.* demonstrates how different catalyst cathodes can interfere with the final product, as the difference in FE and conversion rates were quite significant. The authors also proposed that the guaiacol upgrading was favoured by a chemisorption selectiveness to this compound. This indicates that different feedstocks need different catalytic cathodes to be more effective. Gardew *et al.* exemplified how substrate concentration can affect the FE and selectivity of the product, although it is not a direct relationship. Coke formation was not a major problem, although Zhenglong *et al.* reported finding decanted materials on the cathode chamber.

To avoid the problems related to the commonly used H-type cell, Lister *et al.* proposed a carbon catalyst cathode and DEM as a cheap and effective way to achieve upgrading. Results were promising, and the product had a higher economic value, as it could be used as commodity chemicals, but the authors found that further upgrading would be necessary for utilization as biofuel.

## 6 Plastic recycling

For the creation of a circular plastic economy, the plastic-oil needs to be upgraded into a valuable product, examples include biofuels and feedstock for industry (refined hydrocarbons, petrochemicals, or monomers). To achieve both the calorific values and chemical composition required, heteroatoms (O, S, N, *etc.*) should be removed. Some other elements that are present in the oil were listed in previous sections.

One area where a process of generating feedstock could be helpful includes plastic recycling, where the waste product can be returned to oil and then upgraded. Taking into consideration the highly variable nature of real plastic waste, Kusenberg *et al.* analysed municipal plastic waste and concluded that, to achieve industrial standards, the nitrogen concentration must be reduced by 87.7%, and oxygen by 98.0% (from 825 to 100 and 5200 to 100 ppmw respectively).<sup>73</sup>

Therefore, the focus of the upgrading process is the oxygenated compounds, that is, reducing the O:C ratio of the oil. Oxygenated compounds can lead to lower stability and heating values, as well as a more corrosive product, due to carboxylic acids. Most of the oxygen content comes from PET but to accomplish an effective plastic waste recycling process, PET cannot be excluded. Benzoic acid and its derivatives are the most common carboxylic acids in plastic-oil, and therefore should be the focus of the ECH process.

### 6.1 Selecting a catalytic cathode

Catalysts can be very selective over organic functional groups, and this presents a challenge for the ECH of whole pyrolysis oil

as it is a complex mixture (more than 300 compounds), therefore the cathode needs to be more versatile than the ones chosen for model compounds and be capable of hydrogenating various functional groups. Recent reports shows that catalysts like alloy and carbon–metal hybrids are possible solutions.<sup>74</sup>

Although carboxylic acids are resistant to hydrogenation, ruthenium shows high activity for this process.<sup>75</sup> As shown in the previous section, Ru was also the chosen metal as the cathode for Zhenglong *et al.* (Ru/ACC), Zhang *et al.* (Ru nanoparticles on mesoporous carbon) and Gardew *et al.* (Ru/ACC), which proves its effectiveness in hydrogenating WSBO and phenolic compounds, setting it as a prime candidate for the hydrogenation of whole plastic-oil. The possible mechanism for the hydrogenation of carboxylic acids is shown in Fig. 16.

The hydrogenation of toluene into methylcyclohexane was carried out in a proton exchange membrane (PEM) system by Fukazawa *et al.* and found that PtRu/C was a better catalyst than individual metals such as Pt and Ru and presented high FE (>90%).<sup>53</sup> In a later study, the same group reported on the ECH of benzoic acids into cyclohexane acids (PtRu/C catalyst) and presented high FE (99%) at a current density of 1.5 mA cm<sup>-2</sup>. The authors also reported that in less mild conditions, the carboxyl group could also be hydrogenated (see Fig. 12). As mentioned in previous sections, Du *et al.* also reported on the activity of different cathodes and found that Pt<sub>3</sub>Ru/ACC led to a higher conversion rate than Pt and Ru separately. The authors suggested that this could be the result of a synergistic effect between the two metals, combining platinum's excellent hydrogenation potency and the predominant direct hydrogenolysis ability of ruthenium.<sup>66</sup> In addition, Salakhum *et al.* suggested that combining both metals can facilitate the cleavage of C–O and O–H bonds, as it reduces their heterolytic activation energies.<sup>76</sup> This indicates that PtRu/ACC is a prime candidate for the ECH of carboxylic acids, and therefore, a possible choice of cathode for the hydrogenation of plastic-oil.<sup>52</sup>

### 6.2 Conductivity challenge

The pyrolysis oil has low conductivity values, which is a challenge for an electrochemical process. To circumvent this, an electrolyte is used, as a way of increasing the conductivity. However, the commonly used water-based electrolytes (acid/water; alkali/water and salt/water) are unlikely to be suited for pyrolysis oil treatment, due to the large number of water-insoluble compounds. The removal of both water and the electrolyte (*e.g.*, HCl) after the treatment is also necessary, as it lowers the quality of the product. This would increase the costs and the complexity of the process and could render it unviable.<sup>74</sup>

Possible solutions consist in either increasing oil conductivity *via* additives (*e.g.*, tetrabutylammonium hexafluorophosphate (NBu<sub>4</sub>PF<sub>6</sub>); LiCl; ammonium carbonate) or using a solvent that is capable of dissolving both polar and nonpolar compounds (*e.g.*, ionic liquids, DES (Deep Eutectic Solvents); biomass-derived organic solvents). Studies are necessary to understand the changes in the physicochemical properties of



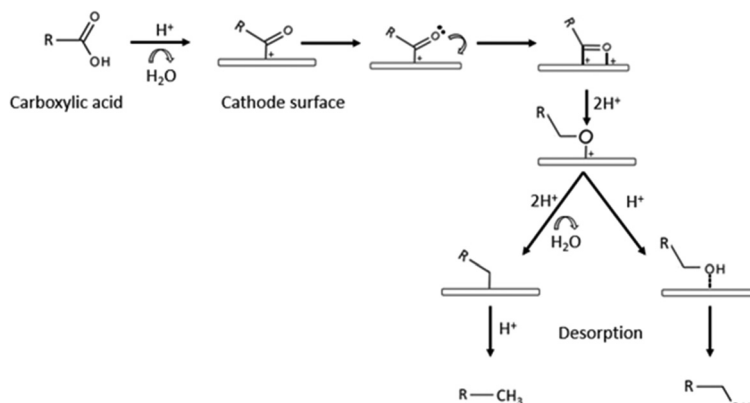


Fig. 16 Mechanism for the hydrogenation of carboxylic acids. Edited with permission from ref. 75. Copyright 2020 Wiley.

the oil and its behavior during ECH that an additive could bring. LiCl could increase the corrosivity of the product as  $\text{Li}^+$  and  $\text{Cl}^-$  are prone to corrosion. Ammonium carbonate could lead to membrane clogging *via* carbonate deposition, as well as increase in the nitrogen composition of the oil, and therefore, its corrosivity.  $\text{NBu}_4\text{PF}_6$  is a chemically inert powder that is commercially available and could provide the much-needed conductivity for the system.

**6.2.1 Ionic liquid and DES.** Ionic liquids and DESs are quite similar in their uses and could serve the same purpose and although DESs, especially natural deep eutectic solvents (NADES), are considered greener and cheaper, it is a very recent class of mixtures and still needs time to develop. Some of its uses are on metallurgy and electrodeposition, due to its high electrical conductivity and solubility, NADES have also been utilized as precursor for biomass processing into more valuable chemicals.<sup>77-79</sup>

**6.2.2 Biomass-derived organic solvents.** Biomass-derived organic solvents are emerging and very promising alternatives as green solvents, that are produced from renewable sources and are non-hazardous to the environment. From this class of

solvents, one of the most prominent is 2-methyltetrahydrofuran (2-MeTHF), which has levulinic acid and furfural, two of bio-oil's main components, as its precursors.<sup>80</sup> That sets both NADES and biomass-derived organic solvents as candidates for alternative solvents for ECH of pyrolysis oils<sup>74</sup> (Fig. 17).

### 6.3 Plastic oil utilization

**6.3.1 Biofuel.** Although not an ideal solution, giving plastic waste a second life usage would be immensely beneficial for the environment as the utilization of the upgraded plastic oil as biofuel could lower the world's consumption of petroleum. For a business-as-usual approach, global plastic waste generation will increase from 260 million tons in 2018 to 460 million tons in 2030. For the same time frame, if the amount of plastic waste collected for recycling achieves 50%, chemical recycling could be responsible for 13% of all plastic production (considering a "high adoption" scenario and oil barrel price around \$75 dollars).<sup>5</sup> This means that 59.8 million tons of plastics would go through pyrolysis, producing approximately 39.0 million tons of plastic oil (65.28 wt% average yield from several plastic pyrolysis reactors as reported by Siu Hua Chang in 2023).<sup>8</sup>

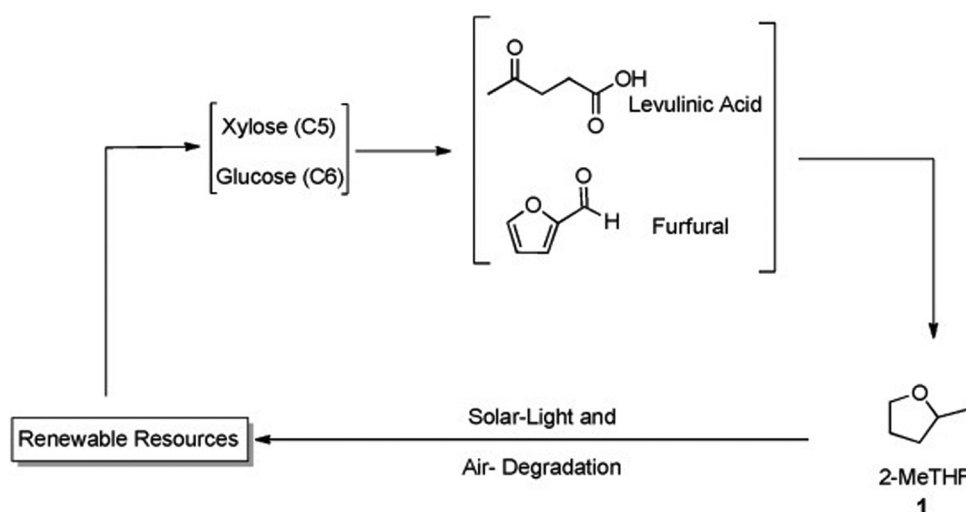


Fig. 17 2-MeTHF production *via* renewable sources. Edited with permission from ref. 80. Copyright 2012 ChemSusChem.



## Biofuel energy production

Total biofuel production is measured in terawatt-hours (TWh) per year. Biofuel production includes both bioethanol and biodiesel.

Our World in Data

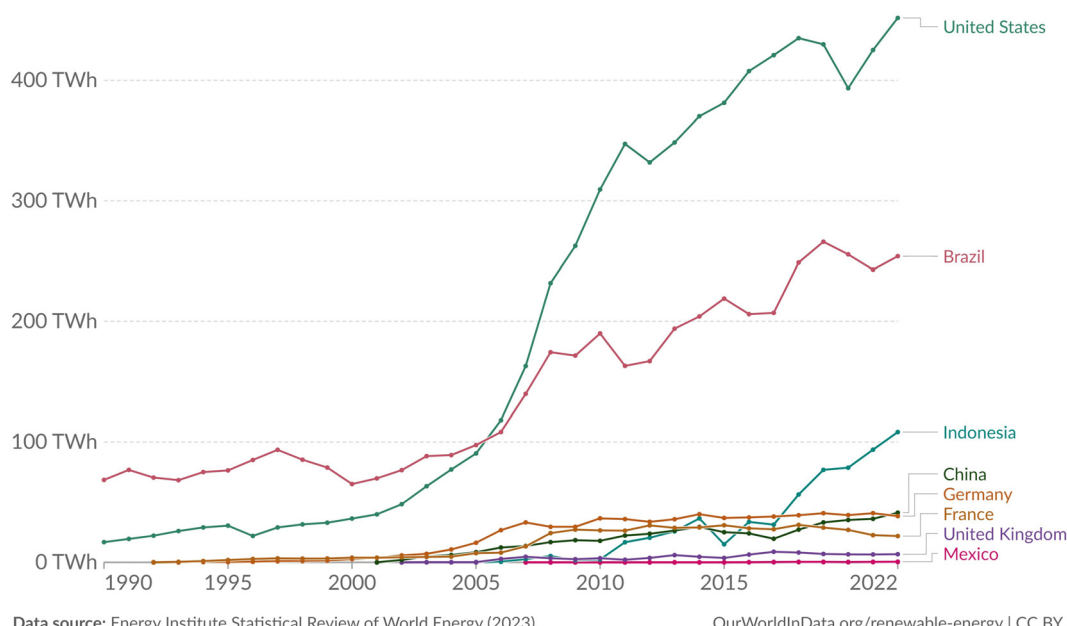


Fig. 18 Total biofuel production in terawatt-hours (TWh) per year. Biofuel production includes both bioethanol and biodiesel. Chart constructed by Our world in data.<sup>83</sup>

As the ECH of plastic oil still needs to be tested, the following calculations will be done using the heating value of the pre-treatment plastic oil ( $41\text{--}47\text{ MJ kg}^{-1}$ , averaged to  $44\text{ MJ kg}^{-1}$ ).<sup>81</sup> This means that approximately  $476.67\text{ TW h}$  (terawatt-hours) per year of biofuel (Fig. 18) could be produced *via* ECH, which is more than the combined production of the whole of Asia, Europe, and Africa in 2021 (approx.  $380\text{ TW h}$ ) and higher than the world's largest producer, the United States ( $399\text{ TW h}$ ).

**6.3.2 Plastic production.** As stated in the previous sections, for the creation of a circular economy, plastic waste needs to be recycled into feedstock for plastic production. In 2019, 368 million tonnes of plastics were produced worldwide<sup>82</sup> 16% of the waste was collected for recycling and, after accounting for losses, 12% went through mechanical recycling. Landfills were the destination for 40%, and incineration for 25%; 19% of all plastic waste produced was mismanaged.<sup>5</sup> This means that, from all the plastic waste, 65% of it, 239.2 million tonnes, was collected but not recycled. If this share went through chemical recycling, 156.15 million tonnes of plastic oil would be produced (65.28 wt% average yield).<sup>8</sup> As the ECH of plastic oil still needs to be tested, three scenarios of conversion rates will be considered: low, fair, and high conversion (50, 75 and 90% respectively). For low conversion rates, 78.08 million tonnes of plastic production feedstock would be produced. Fair and high conversion rates would lead to 117.11 and 140.53 million tonnes respectively. This means that, at the current technology state, up to 38.18% of all resin could come from a sustainable source.

## 7 Conclusions

Fast pyrolysis is a thermochemical process that can be used to produce oil from both biomass and plastic. This material is a complex mixture containing acids, alcohols, aldehydes, esters, phenols, guaiacols, and a great number of other organic compounds. As it has high water content, low C:O ratios, high viscosity, and low density it needs to be upgraded for widespread usage. The electrochemical process for bio-oil upgradation is still new and needs further study to be fully optimized. But previous studies show that it can be done under mild conditions of temperature and pressure. ECH can be done utilizing low-cost materials and can achieve high FE and conversion rates. ECH shows an exciting path for the upgradation process of pyrolysis oils from chemical recycling of both biomass and plastics, a low cost, mild hydrogenation process that can help to achieve the necessary circular and greener economy. The main takeaways from this review are

- Noble metals are reactive species for the ECH of bio-oils. Rh, Pt and Ru loaded carbon cloth have all been reported to hydrogenate alcohols, carboxylic acids, olefins, and aromatic compounds, and presented high efficiency and FE.
- Current, potential, pH, and temperature are all essential factors in the ECH process. The fine tuning of these variables is necessary and directly linked to the quality of the final product.
- Conductivity of the oil presents a major challenge for ECH, alternative electrolytes and additives might be required to make the process viable.



- The hydrogenation of plastic-oils is a possibility that still needs testing, although, as this technology matures, it may become one alternative for both the production of green plastics and biofuels.

## Conflicts of interest

There are no conflicts to declare.

## Acknowledgements

The authors wish to thank UK Engineering and Physical Sciences Research Council (EPSRC) for supporting the work published in the paper through an EPSRC Doctoral Training Partnership Funding.

## References

- 1 THE 17 GOALS|Sustainable Development, Available from: <https://sdgs.un.org/goals>.
- 2 L. Shen and E. Worrell, Plastic Recycling, *Handbook of Recycling: State-of-the-art for Practitioners, Analysts, and Scientists*, 2014, pp. 179–190.
- 3 L. Lebreton and A. Andrade, Future scenarios of global plastic waste generation and disposal, *Palgrave Commun.*, 2019, 5(1), 6.
- 4 G. W. Coates and Y. D. Y. L. Getzler, Chemical recycling to monomer for an ideal, circular polymer economy, *Nat. Rev. Mater.*, 2020, 5(7), 501–516, Available from: <https://www.nature.com/articles/s41578-020-0190-4>.
- 5 T. Hundertmark, M. Mayer, C. Mcnally, T. J. Simons and C. Witte, December 2018, McKinsey on Chemicals, How plastics-waste recycling could transform the chemical industry.
- 6 S. Chawla, B. S. Varghese, C. A. C. G. Hussain, R. Keçili and C. M. Hussain, Environmental impacts of post-consumer plastic wastes: treatment technologies towards eco-sustainability and circular economy, *Chemosphere*, 2022, 308, 135867.
- 7 A. Jahnke, H. P. H. Arp, B. I. Escher, B. Gewert, E. Gorokhova and D. Kühnel, *et al.*, Reducing uncertainty and confronting ignorance about the possible impacts of weathering plastic in the marine environment, *Environ. Sci. Technol. Lett.*, 2017, 4, 85–90, Available from: <https://pubs.acs.org/sharingguidelines>.
- 8 S. H. Chang, Plastic waste as pyrolysis feedstock for plastic oil production: a review, *Sci. Total Environ.*, 2023, 877, 162719, DOI: [10.1016/j.scitotenv.2023.162719](https://doi.org/10.1016/j.scitotenv.2023.162719).
- 9 Q. Zhang, J. Chang, T. Wang and Y. Xu, Review of biomass pyrolysis oil properties and upgrading research, *Energy Convers. Manage.*, 2007, 48(1), 87–92.
- 10 R. Kumar and V. Strezov, Thermochemical production of bio-oil: A review of downstream processing technologies for bio-oil upgrading, production of hydrogen and high value-added products, *Renewable Sustainable Energy Rev.*, 2021, 135, 110152.
- 11 Chemical Recycling 101 [Internet]. [cited 2022 Jul 11], Available from: [https://www.bpf.co.uk/plastipedia/chemical-recycling-101.aspx#\\_edn1](https://www.bpf.co.uk/plastipedia/chemical-recycling-101.aspx#_edn1).
- 12 S. Hansen, A. Mirkouei and L. A. Diaz, A comprehensive state-of-technology review for upgrading bio-oil to renewable or blended hydrocarbon fuels, *Renewable Sustainable Energy Rev.*, 2020, 118, 109548.
- 13 S. Hansen, A. Mirkouei and L. A. Diaz, A comprehensive state-of-technology review for upgrading bio-oil to renewable or blended hydrocarbon fuels, *Renewable Sustainable Energy Rev.*, 2020, 118, 109548.
- 14 V. L. Mangesh, S. Padmanabhan, P. Tamizhdurai and A. Ramesh, Experimental investigation to identify the type of waste plastic pyrolysis oil suitable for conversion to diesel engine fuel, *J. Cleaner Prod.*, 2020, 246.
- 15 M. Kusenberg, M. Roosen, A. Zayoud, M. R. Djokic, H. Dao Thi and S. De Meester, *et al.*, Assessing the feasibility of chemical recycling via steam cracking of untreated plastic waste pyrolysis oils: Feedstock impurities, product yields and coke formation, *Waste Manage.*, 2022, 141, 104–114.
- 16 M. Kusenberg, A. Eschenbacher, M. R. Djokic, A. Zayoud, K. Ragaert and S. De Meester, *et al.*, *Waste Management*, 2022, 138, 83–115, Available from: <https://creativecommons.org/licenses/by-nd/4.0/>.
- 17 Y. Wang, A. Akbarzadeh, L. Chong, J. Du, N. Tahir and M. K. Awasthi, Catalytic pyrolysis of lignocellulosic biomass for bio-oil production: a review, *Chemosphere*, 2022, 297, 134181.
- 18 R. E. Guedes, A. S. Luna and A. R. Torres, Operating parameters for bio-oil production in biomass pyrolysis: a review, *J. Anal. Appl. Pyrolysis*, 2018, 129, 134–149.
- 19 S. Singh, J. P. Chakraborty and M. K. Mondal, Pyrolysis of torrefied biomass: Optimization of process parameters using response surface methodology, characterization, and comparison of properties of pyrolysis oil from raw biomass, *J. Cleaner Prod.*, 2020, 272, 122517.
- 20 Y. Zhang, Y. Liang, S. Li, Y. Yuan, D. Zhang and Y. Wu, *et al.*, A review of biomass pyrolysis gas: forming mechanisms, influencing parameters, and product application upgrades, *Fuel*, 2023, 347, 128461, DOI: [10.1016/j.fuel.2023.128461](https://doi.org/10.1016/j.fuel.2023.128461).
- 21 D. Lachos-Perez, J. C. Martins-Vieira, J. Missau, K. Anshu, O. K. Siakpebru and S. K. Thengane, *et al.*, Review on Biomass Pyrolysis with a Focus on Bio-Oil Upgrading Techniques, *Analytica.*, 2023, 4(2), 182–205.
- 22 J. Zhao, Z. Wang, J. Li, B. Yan and G. Chen, Pyrolysis of food waste and food waste solid digestate: A comparative investigation, *Bioresour. Technol.*, 2022, 354, 127191.
- 23 J. Alvarez, G. Lopez, M. Amutio, J. Bilbao and M. Olazar, Bio-oil production from rice husk fast pyrolysis in a conical spouted bed reactor, *Fuel*, 2014, 128, 162–169.
- 24 J. He, V. Strezov, T. Kan, H. Weldekidan and R. Kumar, Slow pyrolysis of metal(loid)-rich biomass from phytoextraction: characterisation of biomass, biochar and bio-oil, *Energy Proc.*, 2019, 160, 178–185.
- 25 Z. Luo, S. Wang, Y. Liao, J. Zhou, Y. Gu and K. Cen, Research on biomass fast pyrolysis for liquid fuel, *Biomass Bioenergy*, 2004, 26(5), 455–462.



26 F. Stankovikj, A. G. McDonald, G. L. Helms, M. V. Olarte and M. Garcia-Perez, Characterization of the Water-Soluble Fraction of Woody Biomass Pyrolysis Oils, *Energy & Fuels*, 2017, **31**(2), 1650–1664, Available from: <https://www.btg-btl.com/>.

27 K. Sipilä, E. Kuoppala, L. Fagernäs and A. Oasmaa, Characterization of biomass-based flash pyrolysis oils, *Biomass Bioenergy*, 1998, **14**(2), 103–113.

28 A. C. Dyer, M. A. Nahil and P. T. Williams, Catalytic co-pyrolysis of biomass and waste plastics as a route to upgraded bio-oil, *J. Energy Institute*, 2021, **97**, 27–36.

29 H. E. Toraman, T. Dijkmans, M. R. Djokic, K. M. van Geem and G. B. Marin, Detailed compositional characterization of plastic waste pyrolysis oil by comprehensive two-dimensional gas-chromatography coupled to multiple detectors, *J. Chromatogr. A*, 2014, **1359**, 237–246.

30 Ö. Cepelioullar and A. E. Pütün, Products characterization study of a slow pyrolysis of biomass-plastic mixtures in a fixed-bed reactor, *J. Anal. Appl. Pyrolysis*, 2014, **110**(1), 363–374.

31 İ. Çit, A. Sınağ, T. Yumak, S. Uçar, Z. Mısırlıoğlu and M. Canel, Comparative pyrolysis of polyolefins (PP and LDPE) and PET, *Polym. Bull.*, 2010, **64**, 817–834.

32 M. Mariappan, M. S. Panithasan and G. Venkadesan, Pyrolysis plastic oil production and optimisation followed by maximum possible replacement of diesel with bio-oil/methanol blends in a CRDI engine, *J. Cleaner Prod.*, 2021, **312**.

33 D. Xu, S. Yang, Y. Su, L. Shi, S. Zhang and Y. Xiong, Simultaneous production of aromatics-rich bio-oil and carbon nanomaterials from catalytic co-pyrolysis of biomass/plastic wastes and in-line catalytic upgrading of pyrolysis gas, *Waste Manage.*, 2021, **121**, 95–104.

34 K. B. Park, Y. S. Jeong, B. Guzelcifci and J. S. Kim, Two-stage pyrolysis of polystyrene: Pyrolysis oil as a source of fuels or benzene, toluene, ethylbenzene, and xylenes, *Appl. Energy*, 2020, **259**, 114240.

35 I. Kalargaris, G. Tian and S. Gu, Combustion, performance and emission analysis of a DI diesel engine using plastic pyrolysis oil, *Fuel Process. Technol.*, 2017, **157**, 108–115.

36 R. Miandad, M. A. Barakat, A. S. Aburiazaiza, M. Rehan, I. M. I. Ismail and A. S. Nizami, Effect of plastic waste types on pyrolysis liquid oil, *Int. Biodeterior. Biodegradation*, 2017, **119**, 239–252.

37 J. A. Onwudili, N. Insua and P. T. Williams, Composition of products from the pyrolysis of polyethylene and polystyrene in a closed batch reactor: Effects of temperature and residence time, *J. Anal. Appl. Pyrolysis*, 2009, **86**(2), 293–303.

38 I. Graca, J. M. Lopes, H. S. Cerqueira and M. F. Ribeiro, Bio-oils Upgrading for Second Generation Biofuels, *Ind. Eng. Chem. Res.*, 2012, **52**(1), 275–287, Available from: <https://pubs.acs.org/doi/abs/10.1021/ie301714x>.

39 Z. Li, M. Garedew, C. H. Lam, J. E. Jackson, D. J. Miller and C. M. Saffron, Green Chemistry Mild electrocatalytic hydrogenation and hydrodeoxygenation of bio-oil derived phenolic compounds using ruthenium supported on activated carbon cloth, *Green Chem.*, 2012, **14**(9), 2540–2549, Available from: <https://www.rsc.org/greenchem>.

40 T. E. Lister, L. A. Diaz, M. A. Lilga, A. B. Padmaperuma, Y. Lin and V. M. Palakkal, *et al.*, Low-Temperature Electrochemical Upgrading of Bio-oils Using Polymer Electrolyte Membranes, *Energy Fuels*, 2018, **32**(5), 5944–5950.

41 B. Zhang, J. Zhang and Z. Zhong, Low-Energy Mild Electrocatalytic Hydrogenation of Bio-oil Using Ruthenium Anchored in Ordered Mesoporous Carbon, *ACS Appl. Energy Mater.*, 2018, **1**(12), 6758–6763, Available from: <https://pubs.acs.org/sharingguidelines>.

42 Y. Zhou, Y. Gao, X. Zhong, W. Jiang, Y. Liang and P. Niu, *et al.*, Electrocatalytic Upgrading of Lignin-Derived Bio-Oil Based on Surface-Engineered PtNiB Nanostructure, *Adv. Funct. Mater.*, 2019, **29**(10), 1807651, Available from: <https://onlinelibrary.wiley.com/doi/full/10.1002/adfm.201807651>.

43 J. D. Adjaye and N. N. Bakhshi, Catalytic conversion of a biomass-derived oil to fuels and chemicals I: Model compound studies and reaction pathways, *Biomass Bioenergy*, 1995, **8**(3), 131–149.

44 P. M. Mortensen, J. D. Grunwaldt, P. A. Jensen, K. G. Knudsen and A. D. Jensen, A review of catalytic upgrading of bio-oil to engine fuels, *Appl. Catal., A*, 2011, **407**(1–2), 1–19.

45 A. Gutierrez, R. K. Kaila, M. L. Honkela, R. Slioor and A. O. I. Krause, Hydrodeoxygenation of guaiacol on noble metal catalysts, *Catal. Today*, 2009, **147**(3–4), 239–246.

46 Y. H. E. Sheu, R. G. Anthony and E. J. Soltes, Kinetic studies of upgrading pine pyrolytic oil by hydrotreatment, *Fuel Process. Technol.*, 1988, **19**(1), 31–50.

47 W. Baldauf, U. Balfanz and M. Rupp, Upgrading of flash pyrolysis oil and utilization in refineries, *Biomass Bioenergy*, 1994, **7**(1–6), 237–244.

48 J. Wildschut, F. H. Mahfud, R. H. Venderbosch and H. J. Heeres, Hydrotreatment of Fast Pyrolysis Oil Using Heterogeneous Noble-Metal Catalysts, *Ind. Eng. Chem. Res.*, 2009, **48**(23), 10324–10334, Available from: <https://pubs.acs.org/sharingguidelines>.

49 P. T. Williams and P. A. Horne, Characterisation of oils from the fluidised bed pyrolysis of biomass with zeolite catalyst upgrading, *Biomass Bioenergy*, 1994, **7**(1–6), 223–236.

50 A. R. K. Gollakota, M. Reddy, M. D. Subramanyam and N. Kishore, A review on the upgradation techniques of pyrolysis oil, *Renewable Sustainable Energy Rev.*, 2016, **58**, 1543–1568.

51 G. Chen, L. Liang, N. Li, X. Lu, B. Yan and Z. Cheng, Upgrading of Bio-Oil Model Compounds and Bio-Crude into Biofuel by Electrocatalysis: A Review, *ChemSusChem*, 2021, **14**(4), 1037–1052, Available from: <https://onlinelibrary.wiley.com/doi/full/10.1002/cssc.202002063>.

52 A. Fukazawa, Y. Shimizu, N. Shida and M. Atobe, Organic & Biomolecular Chemistry Electrocatalytic hydrogenation of benzoic acids in a proton-exchange membrane reactor, *Org. Biomol. Chem.*, 2021, **19**, 7363–7368.

53 K. Takano, H. Tateno, Y. Matsumura, A. Fukazawa, T. Kashiwagi and K. Nakabayashi, *et al.*, Electrocatalytic



Hydrogenation of Toluene Using a Proton Exchange Membrane Reactor, *Bull. Chem. Soc. Jpn.*, 2016, **89**(10), 1178–1183.

54 Z. Li, S. Kelkar, C. H. Lam, K. Luczek, J. E. Jackson and D. J. Miller, *et al.*, Aqueous electrocatalytic hydrogenation of furfural using a sacrificial anode, *Electrochim. Acta*, 2012, **64**, 87–93.

55 B. Zhao, Q. Guo and Y. Fu, Electrocatalytic Hydrogenation of Lignin-Derived Phenol into Alkanes by Using Platinum Supported on Graphite, *Article Electrochem.*, 2014, **82**(11), 954–959, DOI: [10.5796/electrochemistry.82.954](https://doi.org/10.5796/electrochemistry.82.954).

56 M. Garedew, D. Young-Farhat, J. E. Jackson and C. M. Saffron, Electrocatalytic Upgrading of Phenolic Compounds Observed after Lignin Pyrolysis, *ACS Sustainable Chem. Eng.*, 2019, **7**(9), 8375–8386, Available from: <https://doi.org/10.1021/acssuschemeng.9b00019>.

57 X. H. Chadderton, D. J. Chadderton, J. E. Matthiesen, Y. Qiu, J. M. Carraher and J. P. Tessonner, *et al.*, Mechanisms of Furfural Reduction on Metal Electrodes: Distinguishing Pathways for Selective Hydrogenation of Bioderived Oxygenates Scheme 1. Proposed Pathways of Electrochemical Reduction of Carbonyls in Acidic Electrolytes, *J. Am. Chem. Soc.*, 2017, **139**, 41, Available from: <https://doi.org/10.1021/acscentsuschem.6b00019>.

58 C. H. Lam, C. B. Lowe, Z. Li, K. N. Longe, J. T. Rayburn and M. A. Caldwell, *et al.*, Electrocatalytic upgrading of model lignin monomers with earth abundant metal electrodes, *Green Chem.*, 2015, **17**(1), 601–609, Available from: <https://doi.org/10.1039/C4GC01350A>.

59 W. Liu, W. You, Y. Gong and Y. Deng, High-efficiency electrochemical hydrodeoxygenation of bio-phenols to hydrocarbon fuels by a superacid-noble metal particle dual-catalyst system, *Energy Environ. Sci.*, 2020, **13**, 917.

60 W. Deng, K. Xu, Z. Xiong, W. Chaiwat, X. Wang and S. Su, *et al.*, Evolution of Aromatic Structures during the Low-Temperature Electrochemical Upgrading of Bio-oil, *Energy Fuels*, 2019, **33**(11), 11292–11301, Available from: <https://doi.org/10.1021/acs.energyfuels.9b00019>.

61 A. S. May and E. J. Biddinger, Strategies to Control Electrochemical Hydrogenation and Hydrogenolysis of Furfural and Minimize Undesired Side Reactions, *ACS Catal.*, 2020, **10**(5), 3212–3221.

62 Y. P. Wijaya, T. Grossmann-Neuhaeusler, R. D. Dhewangga Putra, K. J. Smith, C. S. Kim and E. L. Gyenge, Electrocatalytic Hydrogenation of Guaiacol in Diverse Electrolytes Using a Stirred Slurry Reactor, *ChemSusChem*, 2020, **13**(3), 629–639.

63 Y. Kwon and M. T. Koper, Electrocatalytic Hydrogenation and Deoxygenation of Glucose on Solid Metal Electrodes, *ChemSusChem*, 2013, **6**(3), 455–462.

64 A. Roessler, O. Dossenbach and P. Rys, Electrocatalytic Hydrogenation of Indigo, *J. Electrochem. Soc.*, 2003, **150**(1), D1.

65 Y. Song, O. Y. Gutiérrez, J. Herranz and J. A. Lercher, Aqueous phase electrocatalysis and thermal catalysis for the hydrogenation of phenol at mild conditions, *Appl. Catal., B*, 2016, **182**, 236–246.

66 Y. Du, X. Chen and C. Liang, Selective electrocatalytic hydrogenation of phenols over ternary Pt3RuSn alloy. *Molecular Catalysis*, 2023, 535.

67 D. C. Cantu, A. B. Padmaperuma, M. T. Nguyen, S. A. Akhade, Y. Yoon and Y. G. Wang, *et al.*, A Combined Experimental and Theoretical Study on the Activity and Selectivity of the Electrocatalytic Hydrogenation of Aldehydes, *ACS Catal.*, 2018, **8**(8), 7645–7658, Available from: <https://doi.org/10.1021/acscatal.8b00019>.

68 J. A. Lopez-Ruiz, U. Sanyal, J. Egbert, O. Y. Gutiérrez and J. Holladay, Kinetic Investigation of the Sustainable Electrocatalytic Hydrogenation of Benzaldehyde on Pd/C: Effect of Electrolyte Composition and Half-Cell Potentials, *ACS Sustainable Chem. Eng.*, 2018, **6**(12), 16073–16085, Available from: <https://doi.org/10.1021/acscentsuschem.8b00019>.

69 A. Roessler, O. Dossenbach and P. Rys, Electrocatalytic Hydrogenation of Indigo: Process Optimization and Scale-Up in a Flow Cell, *J. Electrochem. Soc.*, 2002, **150**, D1.

70 K. Amouzegar and O. Savadogo, Electrocatalytic hydrogenation of phenol on highly dispersed Pt electrodes, *Electrochim. Acta*, 1994, **39**(4), 557–559.

71 T. S. Dalavoy, J. E. Jackson, G. M. Swain, D. J. Miller, J. Li and J. Lipkowski, Mild electrocatalytic hydrogenation of lactic acid to lactaldehyde and propylene glycol, *J. Catal.*, 2007, **246**(1), 15–28.

72 Z. Li, S. Kelkar, L. Raycraft, M. Garedew, J. E. Jackson, D. J. Miller and C. M. Saffron, A mild approach for bio-oil stabilization and upgrading: electrocatalytic hydrogenation using ruthenium supported on activated carbon cloth, *Green Chem.*, 2014, **16**, 844–852, Available from: <https://doi.org/10.1039/C4GC01350A>.

73 M. Kusenberg, G. C. Faussone, H. D. Thi, M. Roosen, M. Grilc and A. Eschenbacher, *et al.*, Maximizing olefin production via steam cracking of distilled pyrolysis oils from difficult-to-recycle municipal plastic waste and marine litter, *Sci. Total Environ.*, 2022, **838**, 156092.

74 B. Song, F. X. Collard, K. Torr, R. Vellacheri, L. Sandström, *et al.*, IEA Bioenergy Task 34 Report: Electrochemical transformations of fast pyrolysis bio-oils and related bio-oil compounds. International Energy Agency (IEA) Bioenergy Technology Collaboration Programme, 2022, <https://www.ieabioenergy.com/blog/publications/electrochemical-transformations-of-fast-pyrolysis-bio-oils-and-related-bio-oil-compounds/>.

75 M. Tamura, Y. Nakagawa and K. Tomishige, Recent Developments of Heterogeneous Catalysts for Hydrogenation of Carboxylic Acids to their Corresponding Alcohols, *Asian J. Org. Chem.*, 2020, **9**(2), 126–143, Available from: <https://doi.org/10.1002/ajoc.201900667>.

76 S. Salakhum, T. Yutthalekha, S. Shetsiri, T. Witoon and C. Wattanakit, Bifunctional and Bimetallic Pt–Ru/HZSM-5 Nanoparticles for the Mild Hydrodeoxygenation of Lignin-Derived 4-Propylphenol, *ACS Appl. Nano Mater.*, 2019, **2**(2), 1053–1062.

77 A. Paiva, R. Craveiro, I. Aroso, M. Martins, R. L. Reis and A. R. C. Duarte, Natural Deep Eutectic Solvents – Solvents for the 21st Century, *ACS Sustainable Chem. Eng.*, 2014, **2**(5), 1063–1071.



78 E. L. Smith, A. P. Abbott and K. S. Ryder, Deep Eutectic Solvents (DESs) and Their Applications, *Chem. Rev.*, 2014, **114**(21), 11060–11082.

79 B. B. Hansen, S. Spittle, B. Chen, D. Poe, Y. Zhang and J. M. Klein, *et al.*, Deep Eutectic Solvents: A Review of Fundamentals and Applications, *Chem. Rev.*, 2021, **121**(3), 1232–1285.

80 V. Pace, P. Hoyos, L. Castoldi, P. Domínguez de María and A. R. Alcántara, 2-Methyltetrahydrofuran (2-MeTHF): a biomass-derived solvent with broad application in organic chemistry, *ChemSusChem*, 2012, **5**(8), 1369–1379.

81 R. Zevenhoven, M. Karlsson, M. Hupa and M. Frankenhaeuser, Combustion and Gasification Properties of Plastics Particles, *J. Air Waste Manage. Assoc.*, 1997, **47**(8), 861–870, Available from: <https://www.tandfonline.com/action/journalInformation?journalCode=uawm20>.

82 Z. Mańuch, R. Akelytė, M. Camboni and D. Carlander, Chemical Recycling of Polymeric Materials from Waste in the Circular Economy, August 2021, Final Report, Quality Assurance, Project reference/title ECHA/2020/571, Report status, Final report.

83 bp. Statistical Review of World Energy 2022.

